ELSEVIER

Coordination Chemistry Reviews
193–195 (1999) 361–394

COORDINATION CHEMISTRY REVIEWS

www.elsevier.com/locate/ccr

Magnetic clusters from polyoxometalate complexes

Juan M. Clemente-Juan, Eugenio Coronado *

Departamento de Química Inorgánica, Universidad de Valencia, Dr. Moliner 50, 46100 Burjasot, Spain

Received 7 January 1999; accepted 25 May 1999

This paper is dedicated to Professor Boris Tsukevblat on the occasion of his 60th birthday

Contents

* Corresponding author. Tel.: +34-96-3864859; fax: +34-96-3864859.
E-mail address: eugenio.coronado@uv.es (E. Coronado)

PII: S0010-8545(99)00170-8

Abstract

The present article highlights the increasing interest of polyoxometalates in molecular magnetism, providing at the same time a perspective of the state-of-the-art in this area. The main focus is the polyoxotungstates. The first aspect we discuss is that of the coordination chemistry of these metal–oxide ligands. We show that this chemistry leads to remarkable examples of well-insulated magnetic clusters of controlled nuclearity and topology. In these clusters detailed information on the nature of the magnetic exchange interactions can be extracted by using, in addition to the classical magnetic techniques (magnetic susceptibility, magnetization and EPR spectroscopy), other physical techniques as the inelastic neutron scattering (INS) spectroscopy, which provides more direct information on the lower lying energy levels of the magnetic cluster. The second aspect we discuss is that of the interplay between electron delocalization and exchange interactions in the mixed-valence polyoxometalates. We show that these high-nuclearity multielectronic clusters are model systems for the development of new theories in the mixed valence area.

Keywords: Molecular magnetism; Polyoxometalates; Mixed-valence; Magnetic clusters; Magnetic exchange; Electron transfer

1. Introduction

Magnetic clusters, i.e. molecular assemblies formed by a finite number of exchange-coupled paramagnetic centers, are currently receiving much attention in several active areas of research as molecular chemistry, magnetism or biochemistry. As they are in between the small molecular systems and the bulk state, the limited number of interacting centers often allows us to model their properties with quantum mechanical approaches, avoiding the further approximations required to treat extended solids. From this point of view, they serve as model systems for in-depth understanding of the magnetic exchange interactions, providing, at the same time, a testing ground for theories. On the other hand, when these clusters are large enough they enter into the intermediate region of nanoscale magnetic materials where classical and quantum behavior coexist and give rise to unusual magnetic properties as for instance superparamagnetic-like behavior or quantum tunnelling of the magnetization [1]. Organic molecules of increasing sizes and large numbers of unpaired electrons are also being explored as a means of obtaining building blocks for molecule-based magnets [2]. Magnetic clusters of metal ions are also relevant in biochemistry. For example the mixed-valence Fe_4S_4 clusters contained in ferredoxins [3], the manganese clusters present in photosystem II [4], and the magnetic particles of iron found in the storage protein ferritin [5].

A class of inorganic compounds that provide excellent examples of magnetic clusters are the polyoxometalates. These metal–oxide clusters possess a remarkable degree of molecular and electronic tunabilities that impact in disciplines as diverse as catalysis, medicine and materials science [6]. However, the relevance of polyoxometalates in molecular magnetism is an aspect of recent genesis and development

[7]. Two main classes of polyoxometalates are important in this context, the heteropoly anions of tungsten and molybdenum, and the polyoxovanadates.

In the former case the ability of tungstates, and to a less extent of molybdates due to its larger lability and reactivity, to act as ligands toward 3d-transition metal ions leads to the encapsulation by the polyoxometalate framework of a variety of magnetic clusters possessing different spins and showing either ferromagnetic as well as antiferromagnetic exchange couplings. The bulky nonmagnetic polyoxometalate framework guarantees an effective magnetic isolation of the cluster, imposing at the same time its geometry. Furthermore, polyoxometalate chemistry allows the assembly of stable anion fragments into larger clusters. A chemical control of the magnetic nuclearity is therefore possible. The above characteristics make these complexes ideal candidates for modeling the magnetic exchange interactions in clusters of increasing nuclearities and definite topologies [7].

In addition, they can be reversibly reduced to mixed-valence species (heteropoly 'blues' and 'browns') by injection of variable numbers of electrons. In the heteropoly blues these extra electrons are delocalized over a significantly large number of centers of the heteropoly framework [8]. The further introduction into these structures of paramagnetic metal atoms, leads to the creation of clusters in which localized magnetic moments and delocalized electrons can coexist and interact [9]. These features are motivating the development of new theoretical models in order to treat the problem of the electron transfer effects in large clusters, as well as to understand the interplay between electron delocalization, magnetic interactions and Coulomb repulsions in high nuclearity multielectronic systems.

The second important class of magnetic polyoxometalates are the polyoxovanadates(IV). As for the previous systems, polyoxovanadate chemistry provides unique examples to study the exchange interactions as well as the electron delocalization effects in large clusters [10]. In this case, however, the exchange interaction occurs between the addenda vanadium atoms of the polyoxometalate anion. Thus, a polyoxovanadate cluster can be viewed as a fully magnetic cluster in which the $S = 1/2$ spins of the oxovanadium(IV) centers are antiferromagnetically coupled. Then, the intermolecular magnetic interactions are expected to be larger than in the clusters encapsulated by diamagnetic polytungstates. A second difference concerns the electron delocalization. Compared to tungstates and molybdates, the vanadates exhibit, in general, a larger variability in the number of delocalized spins since a fine-tuning of the relative ratio V(V)/V(IV) is sometimes possible. For example, in the $V_{18}O_{42}$ species one can partially oxidize the fully localized V_{18}(IV) cluster by removing up to eight electrons. This has a strong influence on the magnetic properties.

The present review article highlights the increasing interest of polyoxometalates in molecular magnetism, providing, at the same time, a perspective of the state-of-the-art in this area. The main focus is the polytungstates as the magnetism of polyvanadates has recently been reviewed [10]. The first aspect we want to tackle is that of the magnetic clusters encapsulated by these polyoxometalate ligands. We show how polyoxometalate chemistry leads to remarkable examples of well-insulated magnetic clusters of controlled nuclearity and topology for which detailed

information on the nature of the magnetic exchange interactions can be extracted. The second aspect we discuss is that of the interplay between electron delocalization and exchange interactions in mixed-valence polyoxometalates. This part is rather theoretical and focuses upon a question of general interest in molecular magnetism: can electron delocalization control the spin coupling between two widely separated unpaired electrons?

2. Magnetic clusters encapsulated by polyoxotungstate ligands

2.1. Chemical and structural considerations

Two typical heteropolyoxometalate structures having as addenda atoms W and Mo are the so-called α-Keggin structure, α-$[XM_{12}O_{40}]^{n-}$, and the so-called α-Dawson–Wells structure, α-$[X_2M_{18}O_{62}]^{n-}$ (Fig. 1). The Keggin structure involves four three-fold M_3O_{13} groups ('triads'). Each MO_6 octahedron therein is sharing two edges with the two neighboring octahedra and the four triads are attached to one another by corner sharing. This assemblage leads to a central tetrahedral site which is occupied by the heteroatom X. The Dawson–Wells structure can be generated by fusion of two trivacant moieties $[XM_9O_{34}]^{9-}$ coming from the Keggin anion (A-type isomer; see below). These two polyanions can produce the so-called 'lacunary' species wherein one or more addenda atoms have been eliminated along with the terminal oxygen atoms bonded to these addenda. Lacunary species can act as ligands reacting readily with a wide variety of coordinating metal ions to refill the vacant sites. Depending on the way these lacunary species are linked to the coordinating metal ions, different types of magnetic clusters with different nuclearities and structures have been prepared.

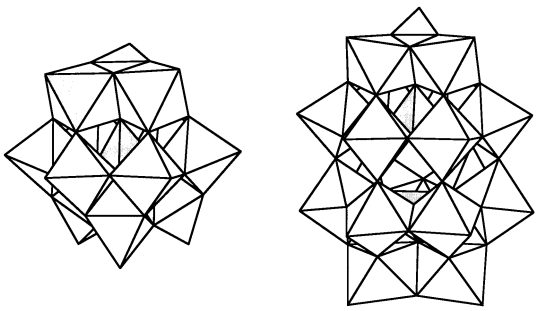

Fig. 1. Structures of two typical heteropoly anions: (a) the α-Keggin structure, α-$[XM_{12}O_{40}]^{n-}$, M = W, Mo; X = $2H^+$, B(III), Al(III), Ga(III), In(III), S(IV), Ge(IV), P(V), As(V), Sb(III), Bi(III), S(VI), Se(IV), Te(IV), Ti(IV), Zr(IV), V(V), Cr(III), Mn(IV), Fe(III), Co(II), Co(III), Cu(II), Cu(I), Zn(II); (b) The α-Dawson–Wells structure, α-$[X_2M_{18}O_{62}]^{n-}$, M = W, Mo; X = P(V), As(V), S(VI).

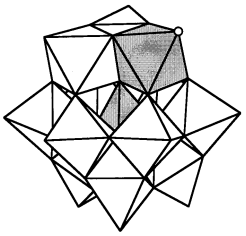

Fig. 2. Structure of the series $[M(H_2O)M'W_{11}O_{39}]^{n-}$ (M = Co(II), Fe(III), Co(III); M′ = Fe(III), Co(II)). Dashed polyhedra represent the magnetic sites. The open circle represents the oxygen atom from a water molecule coordinated to M.

(1) The monovacant Keggin species. This unit has led to the preparation of a series of isomorphous complexes of formula $[M(H_2O)M'W_{11}O_{39}]^{n-}$ (M = Co(II), Fe(III), Co(III); M′ = Fe(III), Co(II)) (Fig. 2). These complexes contain pairs of exchange-coupled metal ions MM′ in two different coordination environments (octahedral and tetrahedral, respectively) sharing a common oxygen atom, as imposed by the heteropoly framework [11].

(2) The trivacant species derived from Keggin and Dawson–Wells structures. By removal of a triad of octahedra sharing edges from α-$[PW_{12}O_{40}]^{3-}$ and α-$[P_2W_{18}O_{62}]^{6-}$ we end up with the trivacant ligands B-$[PW_9O_{34}]^{9-}$ and $[P_2W_{15}O_{56}]^{12-}$ (Fig. 3). These two ligands can act as heptadentate. They can coordinate through six terminal oxygen atoms from six WO_6 octahedra and the unshared terminal oxygen atom from the central heteroatom. In the Keggin anion, however, a group of three WO_6 octahedra sharing corners can also be eliminated giving rise to a ligand formulated as A-$[PW_9O_{34}]^{9-}$, which is hexadentate since in this case the central tetrahedrally coordinated heteroatom does not have any unshared terminal oxygen atom. Let us present the complexes that are obtained using these two kinds of ligands.

The hexadentate A-type $\{PW_9\}$ ligand reacts with divalent Mn, Fe, Ni, Co, Cu, Zn and Pd to give the series of anions $[M_3(PW_9O_{34})_2]^{12-}$ first reported by Knoth et al. [12]. Its structure consists of two A-type $\{PW_9\}$ units connected through a belt of three octahedral metal ions (Fig. 4a). These three metal sites are well separated

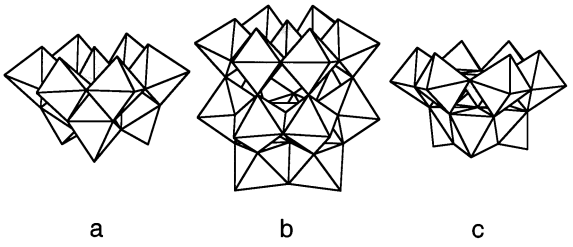

Fig. 3. Trivacant ligands derived from Keggin and Dawson–Wells structures: (a) B-$[PW_9O_{34}]^{9-}$; (b) $[P_2W_{15}O_{56}]^{12-}$; (c) A-$[PW_9O_{34}]^{9-}$.

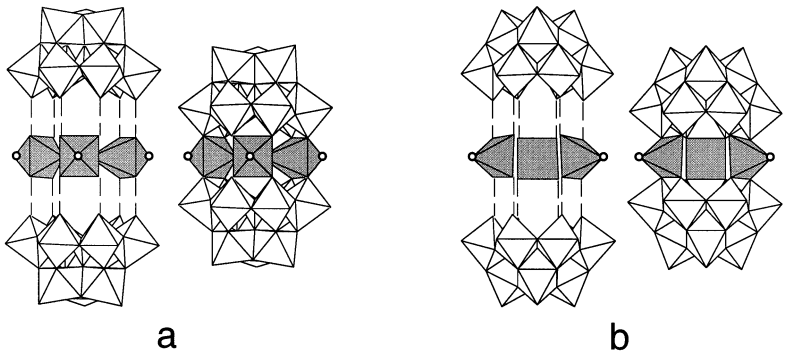

Fig. 4. Structures of the complexes $[Cu_3(H_2O)_3(NO_3)(PW_9O_{34})_2]^{13-}$; (a) and $[Cu_3(H_2O)_2(AsW_9O_{33})_2]^{12-}$ (b).

in the structure creating a central cavity that may be occupied by a small anion as nitrate or nitrite. A related Cu(II) complex was obtained by Hervé et al. from the B-type $\{AsW_9\}$ ligand [13]. In this case, the lone electron pair of the arsenic makes this ligand hexadentate; therefore, it forms a sandwiched complex containing a central Cu(II) triangle wherein two Cu's are pentacoordinated by four oxo groups and a coordinated water, and the third shows a square-planar coordination through four oxo groups (Fig. 4b).

A much more appealing family of magnetic polyoxometalates is furnished by the heptadentate heteropoly ligands B-$\{PW_9\}$ and $\{P_2W_{15}\}$. In both cases extensive series of complexes have been obtained by linking two heteropoly moieties through coordination to a group of four divalent or/and trivalent metal ions. This sandwiched central unit forms a centro-symmetric rhomb-like tetramer $\{M_4O_{16}\}$of four edge-sharing MO_6 octahedra. Two different octahedral sites can be distinguished within the tetrameric unit: the two octahedra of the short diagonal of the rhomb are formed by four oxo groups and two oxygens from the phosphate group; the two octahedra of the long diagonal of the rhomb are formed by four oxo groups, a bridging oxygen from the phosphate group and a terminal oxygen from a coordinated water molecule. The series $[M_4(H_2O)_2(PW_9O_{34})_2]^{10-}$ (Fig. 5), first reported by Tourné et al. in 1973 [14], is known with various divalent metal ions M(II) = Mn, Fe, Ni, Co, Cu and Zn [15–17]. The mixed-valence Mn(II)Mn(III) tetranuclear complex [18] and the Fe(III) complex [19] of this structural type are also known. The related series $[M_4(H_2O)_2(P_2W_{15}O_{56})_2]^{16-}$ (Fig. 6) was also reported for M(II) = Co, Cu and Zn [16], and more recently for M(II) = Mn and Ni [20].

The above complexes have been prepared as sodium or potassium crystalline salts. Interestingly, in some cases a slight variation in the experimental conditions (pH, temperature, time, stoichiometry and concentration of the reagents) leads to the isolation of other polyoxometalate complexes containing magnetic clusters of different nuclearities. The influence of temperature and time can be seen in $[Cu_4(H_2O)_2(PW_9O_{34})_2]^{10-}$. This Cu(II) complex is thermally unstable in solution. In fact, upon heating in boiling water it readily decomposes to give rise to the anion

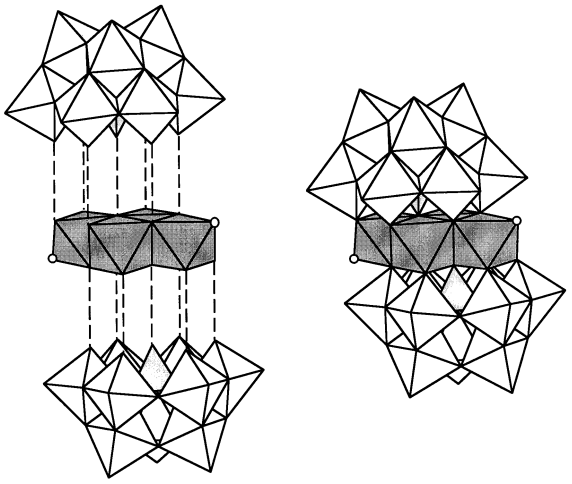

Fig. 5. Structure of the $[M_4(H_2O)_2(PW_9O_{34})_2]^{10-}$ complexes; M(II) = Mn, Fe, Ni, Co, Cu and Zn.

$[PW_{10}Cu_2(H_2O)_2O_{38}]^{7-}$ [21]. This anion exhibits a Keggin structure wherein two Cu(II) have replaced two nearest neighboring W sites giving rise to two kinds of exchange-coupled Cu(II) pairs sharing a corner or an edge (Fig. 7).

The influence of the experimental conditions on the nuclearity of the polyoxometalate cluster is well illustrated in the series of compounds obtained by reaction

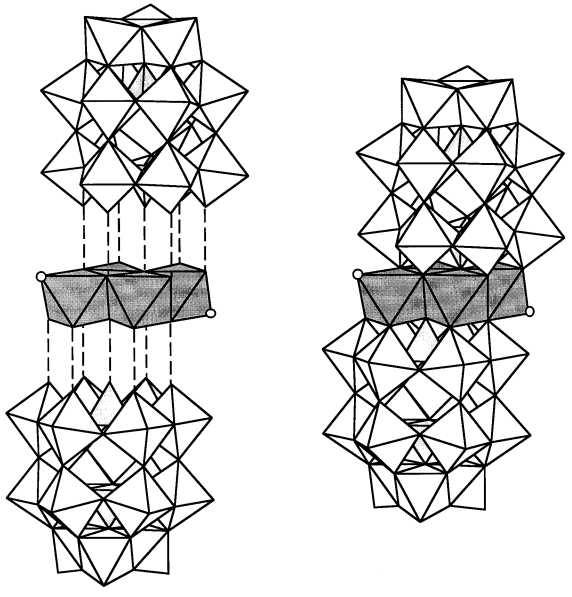

Fig. 6. Structure of the $[M_4(H_2O)_2(P_2W_{15}O_{56})_2]^{16-}$ complexes; M(II) = Mn, Ni, Co, Cu and Zn.

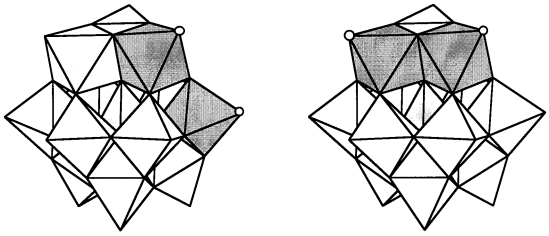

Fig. 7. Structure of the $[PW_{10}Cu_2(H_2O)_2O_{38}]^{7-}$ complex showing the two possible isomers containing neighboring Cu(II) ions.

of B-$\{PW_9\}$ with Ni(II). Thus, up to three different complexes with magnetic Ni(II) clusters of nuclearities 3, 4 and 9 can be isolated when one, two, or three phosphotungstate moieties are linked via their coordination to Ni(II) ions. Although none of the products are obtained exclusively, it is possible to find the best conditions to crystallize in high yield the salt of the desired nickel complex [22]. The Ni_3 cluster is present in the $[Ni_3(H_2O)_3(PW_{10}O_{39})H_2O]^{7-}$ polyoxoanion (Fig. 8). This polyoxoanion may be viewed as a reconstituted Keggin-like structure $\{PNi_3W_9O_{40}\}$ wherein a W_3 triad has been substituted by Ni_3. Therefore, this triangular Ni_3 cluster is formed by three edge-sharing NiO_6 octahedra [23]. The Keggin structure has an additional cap of WO_6 that produces a distorted $[Ni_3WO_4]$ cubane-type core with the Ni_3 cluster. Within the cluster each NiO_6 octahedron contains four oxide ions, a bridging oxygen from the central phosphate group, and a terminal oxygen from a coordinated water molecule. The Ni_4 cluster exhibits the typical structure of the series $[M_4(H_2O)_2(PW_9O_{34})_2]^{10-}$. Finally, the Ni_9 cluster is obtained by condensation of three reconstituted Keggin anions $\{PNi_3W_9O_{40}\}$. In the resulting giant polyoxometalate complex $[Ni_9(OH)_3(H_2O)_6(HPO_4)_2(PW_9O_{34})_3]^{16-}$ (Fig. 9) the magnetic cluster is formed by

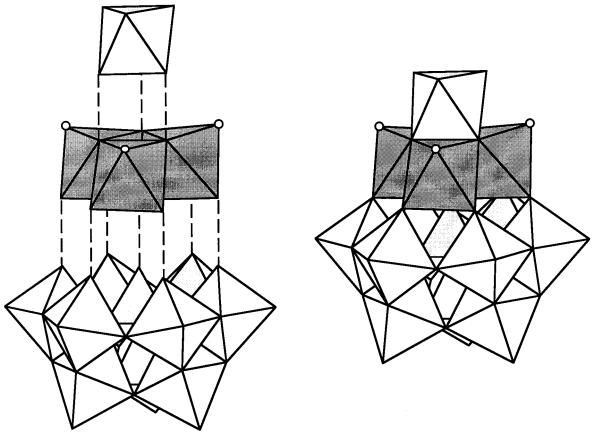

Fig. 8. Structure of the $[Ni_3(H_2O)_3(PW_{10}O_{39})H_2O]^{7-}$ complex.

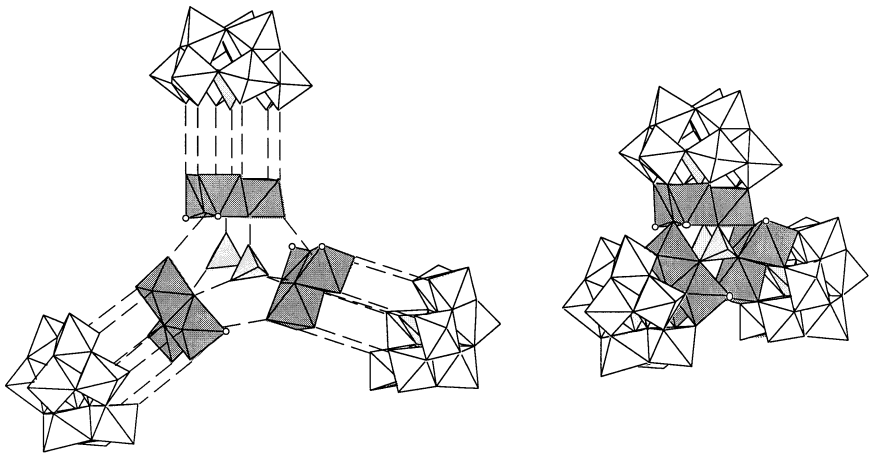

Fig. 9. Structure of the $[M_9(OH)_3(H_2O)_6(HPO_4)_2(PW_9O_{34})_3]^{16-}$ complexes; M(II) = Co, Ni.

three triangular Ni_3O_{13} units sharing edges. These triangles are connected to each other by three OH^- bridging groups and two central HPO_4^{2-} groups in order to form a triangle of triangles. The periphery of this polyoxoanion is formed by three diamagnetic ligands $(PW_9O_{34})^{9-}$ which guarantee the insulation of the magnetic clusters. As for Ni_3 and Ni_4, in the Ni_9O_{36} unit the terminal oxygens of the NiO_6 octahedra belong to coordinated water molecules. The analogous nonanuclear cluster of cobalt(II) is also known. It was identified by Weakley as a by-product (ca. 5%) in the preparation of $[Co_4(H_2O)_2(PW_9O_{34})_2]^{10-}$ [24].

In the previous paragraph we have shown that a successful strategy to vary the nuclearity of the magnetic clusters is that of condensing several Keggin units. A second possibility is that of replacing the P heteroatom of the central tetrahedral site of the Keggin unit by a paramagnetic metal cation. This can be illustrated in the structural type provided by the $[M_4(H_2O)_2(PW_9O_{34})_2]^{10-}$ series. An increase in the magnetic nuclearity from 4 to 5 or 6 can then be achieved. Examples of magnetic clusters of nuclearity 5 are found in the series of chiral polytungstometalates $[WM_3(H_2O)_2(M'W_9O_{34})_2]^{12-}$ discovered by Tourné et al. [25]. These $M_3M'_2$ anions are formed on ageing concentrated solutions of sodium salts of the polyanions $[M(H_2O)M'W_{11}O_{39}]^{8-}$ (MM′ = Co(II)Co(II) and Zn(II)Zn(II)). In this series the octahedral site, M, can also be Mn(II) or Mn(III), Fe(II) or Fe(III), Co(III), Ni(II), Cu(II), Pd(II) and V(IV). Their structure is analogous to that of the $[M_4(H_2O)_2(PW_9O_{34})_2]^{10-}$ series (Fig. 10a). Like these anions, they contain similar B-$\{XW_9\}$ trivacant fragments of the α-Keggin-type anion (where X = M′ = Co(II) and Zn(II)). The important difference is that in this series one of the four metal sites forming the central rhomb-like cluster is occupied by a non-magnetic tungsten atom. On the other hand, since the tetrahedral site can be either occupied by Zn(II) (diamagnetic) or Co(II) (paramagnetic), the nuclearity of the magnetic cluster can be varied from 3 to 5. A feature that should add magnetic interest to this series is

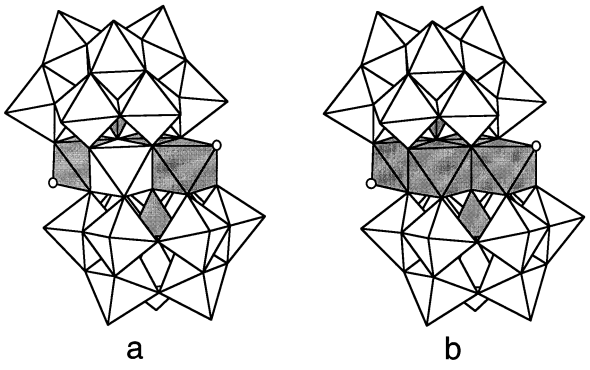

Fig. 10. (a) Structure of the $[WM_3(H_2O)_2(M'W_9O_{34})_2]^{12-}$ complex (M = Co(II), Zn(II), Mn(II) or Mn(III), Fe(II) or Fe(III), Co(III), Ni(II), Cu(II), Pd(II) and V(IV); M′ = Co(II) and Zn(II). (b) Structure of the $[Fe_2Cu_2(H_2O)_2(FeW_9O_{34})_2]^{12-}$ complex.

the possibility of having bimetallic magnetic clusters, since the magnetic ions accommodated in the two metal sites can be different. Finally, an example of magnetic cluster of nuclearity 6 is also known. It was reported by Wasfi et al. in the polyanion formulated as $[Fe_2Cu_2(H_2O)_2(FeW_9O_{34})_2]^{12-}$ [26]. This anion contains a bimetallic central cluster $Fe(III)_2Cu(II)_2$ of edge-sharing octahedra wherein the two Cu(II) ions are occupying the hydrated positions; the two remaining Fe(III) ions are located at the tetrahedral sites and connected to the central tetrameric cluster through an oxo bridge (Fig. 10b). Subsequently, we present a magnetic characterization of the aforementioned clusters grouped according to their nuclearities

2.2. Dimeric clusters

2.2.1. The series $[M(H_2O)M'W_{11}O_{39}]^{n-}$ (M = Co(II), Fe(III); M′ = Co(II), Fe(III), Co(III))

Magnetic studies on this series of isomorphous heteropoly complexes were reported in 1972 by Baker and co-workers [11]. In these works the potential of polyoxometalate chemistry for providing examples of exchange-coupled clusters was already advanced. The authors investigated the exchange interactions between MM′ pairs of differing paramagnetic ions by studying the magnetic susceptibility over the temperature range 2–300 K of the potassium salts of these heteropoly complexes. Four magnetic pairs were studied namely Co(II)Co(II), Co(II)Fe(III), Fe(III)Co(II) and Fe(III)Co(III). All exhibited antiferromagnetic exchange interactions in the range -2 to -25 cm^{-1}.

In order to obtain a much deeper and more detailed insight into the nature of the magnetic coupling in these systems we have used the Inelastic Neutron Scattering (INS) technique. This spectroscopic technique was introduced by Güdel and Furrer in 1977 to study magnetic clusters [27]. These authors showed that INS provides a direct access to the split energy levels of the electronic ground state of the cluster caused by exchange interactions. Therefore, it is a valuable and advantageous

complement to the bulk magnetic techniques (magnetic susceptibility and specific heat) that only provide indirect—and often insufficient—information on the energy spectrum. However, the applicability of INS is limited by the large amounts of sample needed (10–20 g) and by the presence of hydrogen atoms. These limitations have seriously restricted the use of INS in coordination chemistry. In this respect, magnetic polyoxometalates are quite suitable as large amounts of fully deuterated samples of their salts can be available easily. This possibility prompted us to undertake, in collaboration with Güdel's group, an INS study on some relevant magnetic clusters of this kind of nuclearities two and four. Among the dimeric clusters of the present series we have studied the Co(II)Co(II) complex [28]. This dimer is of special interest because high-spin octahedral Co(II) has an orbitally degenerate ground state $^4T_1$. Thus, it has enabled the study of exchange interactions in the presence of orbital degeneracy, that is an open problem in magnetism for which no general theory is available. In the present case an anisotropic exchange Hamiltonian has been assumed to be the most appropriate:

$$H = -2J_z S_{z1} S_{z2} - 2J_{xy}(S_{x1} S_{x2} + S_{y1} S_{y2}) \quad (1)$$

In this expression S_1 is the spin associated with the orbitally non degenerate ground state of the tetrahedral Co(II), $^4A_2$, which is well described as a spin-only $S_1 = 3/2$, while S_2 represents an effective spin 1/2 associated to the lowest Kramers doublet of the octahedral Co(II). This anisotropic spin doublet results from the splitting into six Kramers doublets of the $^4T_1$ ground state caused by the combined effect of spin-orbit coupling and distortion from octahedral symmetry [29]. INS spectra recorded at temperatures at which the lowest Kramers doublet is the only significantly populated (below 30 K), clearly shows that a fully-isotropic Heisenberg model (with $J_z = J_{xy}$) is too simplistic to reproduce the results and that anisotropy is important. In fact up to four magnetic excitations from the ground spin level to the excited ones have been observed at 1.15, 4.1, 5.7 and 7 meV (1 meV = 8.0655 cm^{-1}), that are conveniently reproduced from the above exchange Hamiltonian to give an antiferromagnetic exchange interaction $J_z = -17.9$ cm^{-1} and an amount of exchange anisotropy, defined as the ratio J_{xy}/J_z, equal to 0.33. The parameters are listed in Table 1. This J_{xy}/J_z value is intermediate between the fully-anisotropic Ising coupling ($J_{xy}/J_z = 0$) and the fully-isotropic Heisenberg coupling ($J_{xy}/J_z = 1$). This set of parameters leads to a ground spin state formed by a mixture of $|1 \pm 1>$ and $|2 \pm 1>$ wave functions, expressed in the $|SM>$ basis, where S is the total spin and M its z-projection (Fig. 11a). Notice that this energy-level pattern provides intensity to the four observed excitations, as the selection rules for magnetic INS are $\Delta S = 0, \pm 1$ and $\Delta M = 0, \pm 1$. This is definite proof for the presence of significant exchange anisotropy in this cobalt dimer. Interestingly, the magnetic behavior, which is largely insensitive to the exchange anisotropy, is closely reproduced from the anisotropic exchange parameters derived from INS (Fig. 11b).

Table 1
Magnetic characterization of magnetic clusters coordinated by polyoxotungstate ligands. N and S_i are the magnetic nuclearitity of the cluster and the local spin values of the interacting metal centers

Polyoxometalate	Magnetic cluster	N	S_i	Magnetic parameters (cm^{-1})	Comments	Ref.
$[Co(H_2O)CoW_{11}O_{39}]^{8-}$	$Co(II)_2O_9$	2	3/2 and '1/2'[a]	$J_z = -17.9$, $J_{xy}/J_z = 0.33$	AF exchange, aisotropic model ($J_z \neq J_{xy}$)	[29]
$[PW_{10}Cu_2(H_2O)_2O_{38}]^{7-}$	$Cu(II)_2O_{11}Cu(II)_2O_{10}$	2	1/2	$J = -7.6$, $J = -3.6$	AF exchange Heisenberg model	[22]
$[Cu_3(H_2O)_2(AsW_9O_{33})]^{12-}$	$Cu(II)_3O_{14}$	3	1/2	$J = -2.6$	AF exchange, Heisenberg model	[31,32]
$[Ni_3(H_2O)_3(PW_{10}O_{39})H_2O]^{7-}$	$Ni(II)_3O_{13}$	3	1	$J = 3.9$, $D = 5.8$	F exchange, Heisenberg model + SIA[b]	[23,24]
$[Cu_4(H_2O)_2(PW_9O_{34})_2]^{10-}$	$Cu(II)_4O_{16}$	4	1/2	$J = -3.5$, $J' = -12.5$	AF exchange, Heisenberg model	[34,35]
$[Mn_4(H_2O)_2(PW_9O_{34})_2]^{10-}$	$Mn(II)_4O_{16}$	4	5/2	$J = -1.7$, $J' = -0.3$	AF exchange, Heisenberg model	[17,20]
$[Ni_4(H_2O)_2(PW_9O_{34})_2]^{10-}$	$Ni(II)_4O_{16}$	4	1	$J = 6.5$, $J' = 2.5$, $D = 4.5$	F exchange, Heisenberg model + SIA[b]	[20,23]
$[Co_4(H_2O)_2(PW_9O_{34})_2]^{10-}$	$Co(II)_4O_{16}$	4	'1/2'[a]	$J_z = 12$, $J'_z = 19$, $J_{xy}/J_z = 0.60$	F exchange, Anisotropic model ($J_z \neq J_x \neq J_y$)	[34–39]
$[Fe_4(H_2O)_2(PW_9O_{34})_2]^{10-}$	$Fe(II)_4O_{16}$	4	2	–	F exchange	[7]
$[WCo_3(H_2O)_2(CoW_9O_{34})_2]^{12-}$	$Co(II)_5O_{18}$	5	'1/2'[a]	$J_z = 12.9$, $J_{xy}/J_z = 0.43$, $J'_z = -10.0$, $J'_{xy}/J'_z = 0.33$	Coexistence of F and AF exchange, anisotropic model ($J_z \neq J_{xy}$)	[41]
$[Fe_2Cu_2(H_2O)_2(FeW_9O_{34})_2]^{10-}$	$Fe(III)_4Cu(II)_2O_{36}$	6	5/2 and 1/2	–	AF exchange	[27]
$[Co_9(OH)_3(H_2O)_6(HPO_4)_2(PW_9O_{34})_3]^{16-}$	$Co(II)_9O_{36}$	9	'1/2'[a]	$J_z = 8.4$, $J'_z = -12$	Coexistence of F and AF exchange, Ising model ($J_z \neq 0$; $J_x = J_y = 0$)	[40]
$[Ni_9(OH)_3(H_2O)_6(HPO_4)_2(PW_9O_{34})_3]^{16-}$	$Ni(II)_9O_{36}$	9	1	$J = 3.9$, $J' = -1.4$	Coexistence of F and AF exchange, Heisenberg model	[23]

[a] Effective spin for octahedral Co(II).
[b] Single-ion anisotropy.

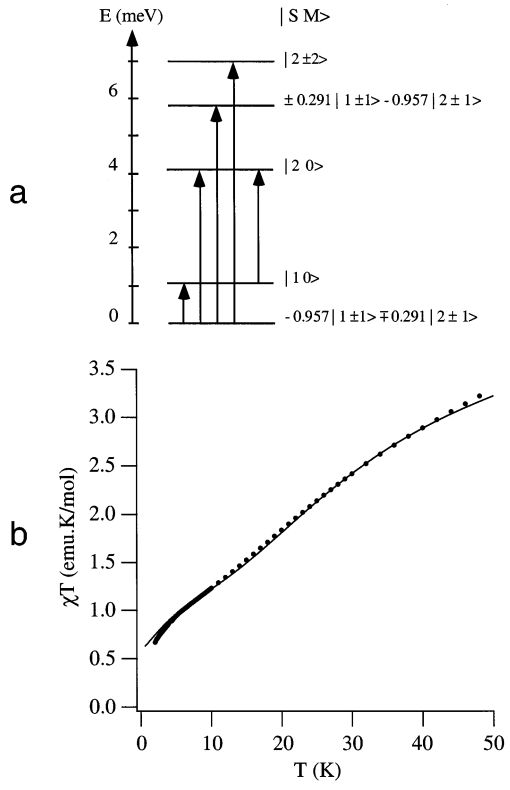

Fig. 11. The complex $[Co(II)(H_2O)Co(II)W_{11}O_{39}]^{8-}$: (a) energy levels and magnetic excitations observed by INS spectroscopy; (b) low temperature magnetic behavior. The solid line represents the theoretical curve calculated from the parameters derived from INS (Table 1).

2.2.2. The complex $[PW_{10}Cu_2(H_2O)_2O_{38}]^{7-}$ [21]

This heteropoly complex was prepared as a mixed potassium/sodium salt. As we have pointed out above, the single-crystal X-ray diffraction study indicated that this anion exhibits an α-Keggin structure wherein two Cu(II) ions have replaced two W sites. However, given the high symmetry of the unit cell (F cubic cell), the X-ray diffraction study was completely unable to locate the two Cu atoms, which appeared fully disordered over the 12 possible locations in each anion structure. In this case, magnetic susceptibility and EPR spectroscopy were a good complement as these magnetic techniques allowed us to locate the two Cu atoms on neighboring sites of the Keggin structure, giving rise to two isomers wherein the CuO_6 octahedra share a corner or an edge.

Thus, the magnetic susceptibility shows a rounded maximum centered at $T \approx 6$ K consistent with the presence of antiferromagnetically coupled pairs in the heteropoly complex (Fig. 12a). A fit of these data clearly indicate the presence of similar amounts of two kinds of Cu(II) pairs. The resulting values for the exchange couplings are -7.6 and -3.2 cm^{-1}. On the other hand, this fit indicates that only

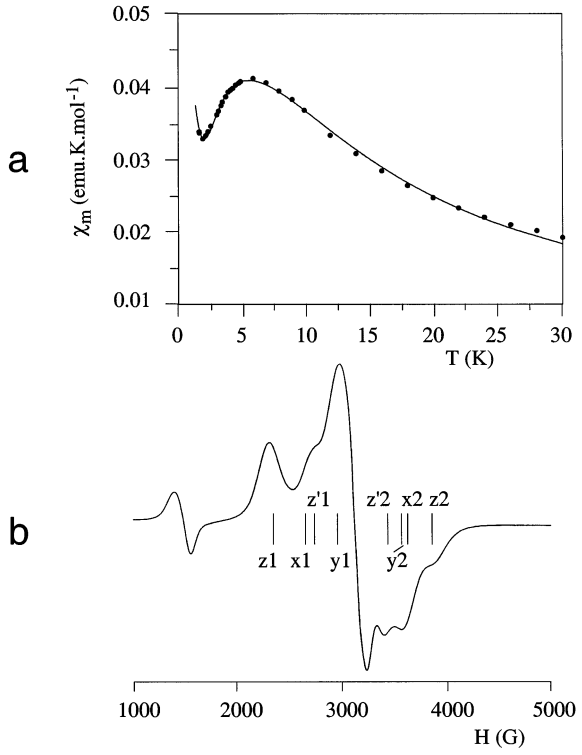

Fig. 12. Magnetic properties of the $[PW_{10}Cu_2(H_2O)_2O_{38}]^{7-}$ complex: (a) thermal dependence of the magnetic susceptibility; (b) powder EPR spectrum recorded at 4.2 K showing the position of the bands obtained by the simulation to two anisotropic spin triplets.

a small proportion of Keggin units contain nonadjacent (magnetically uncoupled) Cu's ($\sim 8.5\%$). In view of the larger Cu–O–Cu bridging angle shown by the isomer in which the Cu dimer is sharing a corner (148° compared to 125.5°), the strongest antiferromagnetic coupling ($J = -7.6$ cm^{-1}) has been associated with this isomer, while the weaker one ($J = -3.2$ cm^{-1}) has been associated with the isomer containing the edge-sharing Cu dimer. EPR spectra recorded at 4 K are also in agreement with this picture as they showed the typical features of two independent spin triplets with two different spin anisotropies ($|D| = 0.076$ and 0.03 cm^{-1}), which have to be associated with the two types of exchange-coupled Cu pairs (Fig. 12b).

2.3. Trimeric clusters

2.3.1. The complex $[Cu_3(H_2O)_2(AsW_9O_{33})_2]^{12-}$

The magnetic susceptibility and EPR properties of this complex were reported by Kokoszka et al. [30]. The magnetic cluster is formed by a nearly equilateral triangle (Cu–Cu distances = 4.707 and 4.669 Å) of Cu ions encapsulated by two polyoxo-

tungstate anions. Accordingly, an isotropic exchange Hamiltonian that considers a single Cu–Cu pairwise interaction, J, was assumed to describe the magnetic properties:

$$H = -2J(S_1S_2 + S_2S_3 + S_3S_1) \quad (2)$$

When the coupling is antiferromagnetic this Hamiltonian leads to an energy diagram formed by two degenerate doublets $S = 1/2$ and a quartet excited state $S = 3/2$ separated by an energy $|3J|$. Trimeric clusters of this kind attracted interest in magnetism because they are the next simplest case after dimers for which the lack of a molecular inversion center permits an antisymmetrical exchange term ($dS_1 \times S_2$) to enter into the spin Hamiltonian. However, experimental verification of this interaction in the present example was not possible. Thus, the magnetic susceptibility was interpreted with an antiferromagnetic coupling $J = -2.6$ cm^{-1}, which places the $S = 3/2$ state about 8 cm^{-1} above the two $S = 1/2$ states. The resolved fine structure of the $S = 3/2$ state observed by EPR [31] was evidence of the good insulation of these triangular clusters.

2.3.2. The complex $[Ni_3(H_2O)_3(PW_{10}O_{39})H_2O]^{7-}$

This complex exhibits a unique structure, only found for nickel, that contains a triangular Ni_3 cluster formed by three edge-sharing NiO_6 octahedra (Fig. 8). The magnetic properties of this cluster are largely due to interactions between $^3A_2$ nickel(II) ions. As can be seen in the plot of the product χT (proportional to the square of μ_{eff}), which exhibits a gradual increase as the temperature is decreased and a maximum at $T = 8$ K, the Ni – Ni pairwise interactions between the spins $S = 1$ are ferromagnetic leading to a high ground spin state $S = 3$ for the cluster (Fig. 13). This result was not unexpected as the structure of the cluster shows

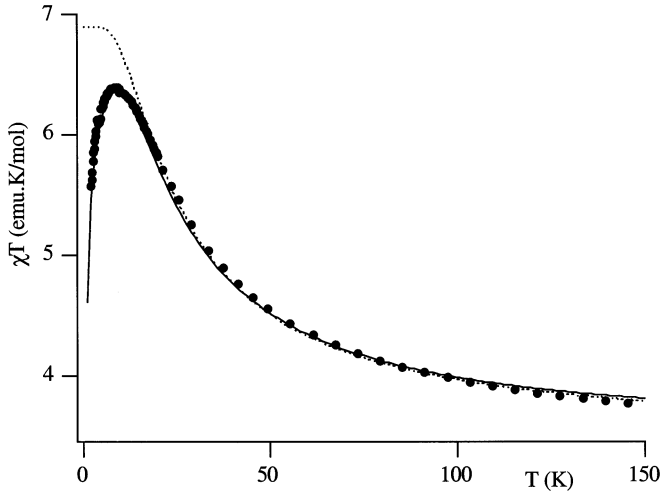

Fig. 13. Magnetic behavior of the $[Ni_3(H_2O)_3(PW_{10}O_{39})H_2O]^{7-}$ complex. Dotted line represents the best fit to the isotropic Heisenberg exchange model. Solid line represents the best fit to a model that also considers a single-ion anisotropy term. The resulting parameters are given in the text and in Table 1.

Ni–O–Ni angles comprised between 90 and 100°, which are in the range in which the Ni–Ni ferromagnetic exchange pathways are dominant [32]. The magnetic properties were initially analyzed assuming a Heisenberg exchange Hamiltonian (Eq. (2)) [23]. This model gave a good description of the magnetic data above the maximum in χT. However, to account for the decrease in $\chi_m T$ observed at lower temperatures, an axial single-ion anisotropy of the type DS_{iz}^2, where D represents the zero-field splitting parameter of the local spin $S = 1$, has been added to the spin Hamiltonian [22]. An excellent reproduction of the experimental data is then obtained with a ferromagnetic exchange $J = 3.9\ cm^{-1}$ and a ZFS parameter $D = 5.8\ cm^{-1}$ (solid line in Fig. 13; Table 1).

2.4. Tetrameric clusters: the series $[M_4(H_2O)_2(PW_9O_{34})_2]^{10-}$ and $[M_4(H_2O)_2(P_2W_{15}O_{56})_2]^{16-}$ (M = Mn(II), Cu(II), Co(II), Ni(II) and Fe(II))

The two series of heteropoly complexes $[M_4(H_2O)_2(PW_9O_{34})_2]^{10-}$ and $[M_4(H_2O)_2(P_2W_{15}O_{56})_2]^{16-}$ have furnished the largest variety of tetrameric magnetic clusters M_4O_{16}, wherein the size and nature of the interacting magnetic moments as well as the sign of the exchange interactions can be varied by changing the transition metal ions. Thus, Mn(II), Ni(II) and Cu(II) possess orbitally non degenerate ground spin states ($S = 5/2$, 1 and 1/2, respectively) whose interactions are well described by an isotropic Heisenberg Hamiltonian:

$$H = -2J(S_1S_3 + S_1S_4 + S_2S_3 + S_2S_4) - 2J'S_1S_2 \quad (3)$$

where J and J' refer to the two types of magnetic interactions associated with the sides and short diagonal of the rhomb according to the numbering scheme indicated in Fig. 14. In contrast high-spin octahedral Co(II) and Fe(II) have orbitally degenerate ground states that should cause the appearance of an effective exchange anisotropy, preventing the use of the simple Heisenberg spin Hamiltonian to treat the magnetic properties of these clusters. In all cases the magnitude of the exchange values is expected to be relatively small, as near 90° superexchange paths through the bridging oxo groups are involved. Focusing now on the sign of the exchange interactions, it has been found that Cu(II) and Mn(II) clusters exhibit weak antiferromagnetic interactions, while Ni(II), Co(II) and Fe(II) clusters are ferromagnetic. It should be noted that for a given magnetic cluster, the magnetic

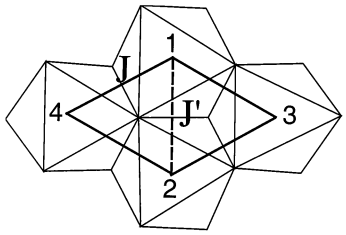

Fig. 14. Exchange network in the tetrameric magnetic clusters M_4O_{16} of the series $[M_4(H_2O)_2(PW_9O_{34})_2]^{10-}$ and $[M_4(H_2O)_2(P_2W_{15}O_{56})_2]^{16-}$.

behaviors of Keggin and Dawson–Wells derivatives are coincident within experimental error. This observation agrees with the fact that the structural features of the cluster are maintained when one pass from Keggin to Dawson–Wells derivatives. Therefore, it seems convenient to divide the presentation of these compounds according to the sign of the exchange interactions.

2.4.1. Antiferromagnetic clusters

The magnetic behaviors of Cu and Mn complexes are reported in Fig. 15. In both cases the χT product decreases when the temperature is decreased, in agreement with the presence of antiferromagnetic interactions between the metal ions of the tetrameric clusters. They can be well-reproduced by using a Heisenberg spin Hamiltonian (Eq. (3)) [17,20,33,34]. The final exchange parameters are summarized in Table 1. It should be noted, however, that these behaviors sharply differ at low temperatures. Thus, while in the Mn_4 cluster χT vanishes when the temperature approaches absolute zero, the Cu_4 cluster reaches a plateau of 0.86 emu K mol^{-1} below 6 K. This difference indicates that even though the exchange interactions are antiferromagnetic in both cases, their spin ground states are different, being magnetic for Cu_4 and nonmagnetic for Mn_4. This has been attributed to the presence of spin frustration. In fact, the topology of the cluster is such that the interacting spins are under the influence of two competing antiferromagnetic interactions J and J', that tend to orient them in different directions [35]. Under these circumstances the ground spin state will depend on the ratio J'/J. When the exchange through the diagonal of the rhomb, J', is sufficiently small compared to that through the sides, J, the ground state is the antiferromagnetic one (i.e. $S=0$), as observed in the Mn_4 cluster where $J'/J=0.18$. In turn, when the diagonal exchange interaction dominates, the spin frustration leads to the stabilization of an intermediate-spin ground state. This is the situation in the Cu_4 cluster for which the large value of the ratio J'/J ($=3.6$) leads to a ground state that contains the spin $S=1$ (Fig. 16a). The EPR spectrum at 4.2 K has confirmed the nature of this magnetic ground state (Fig. 16b). Thus, the spectrum is typical of a spin-triplet with small values of the zero-field splitting parameters ($|D|=0.032$ cm^{-1}; $E/D=-0.17$).

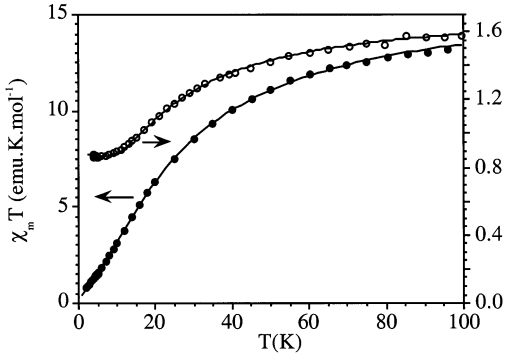

Fig. 15. Magnetic behavior of the Mn(II) (open circles) and Cu(II) (filled circles) complexes of the series $[M_4(H_2O)_2(PW_9O_{34})_2]^{10-}$. Solid lines represent the best fit to the Heisenberg exchange model. The resulting parameters are given in Table 1.

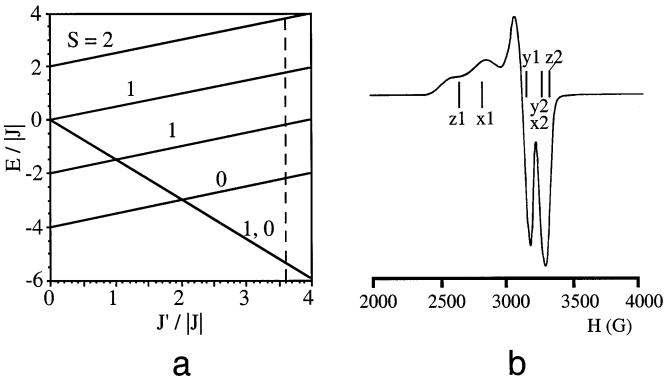

Fig. 16. (a) Energies of the spin states of a rhomb-like cluster of antiferromagnetically coupled $S = 1/2$ spins as a function of the J'/J ratio. Dashed line corresponds to the J'/J value found for the Cu_4O_{16} cluster; (b) powder EPR spectrum of the Cu_4O_{16} cluster recorded at 4.2 K showing the typical features of a spin triplet.

The smaller (absolute) value of J' compared to J in the Mn_4 cluster may be correlated to the larger Mn–Mn distance for the diagonal of the rhomb (3.45 Å compared to 3.29 Å for the side of the rhomb). The reversal of this situation in the Cu_4 cluster is a consequence of the Jahn–Teller distortion of the CuO_6 sites, which are axially distorted in such a way than the long axes of the four octahedra are parallel; as a result, the Cu–Cu distance for the diagonal of the rhomb is shorter (3.08 Å compared to 3.25 Å).

2.4.2. Ferromagnetic clusters

The magnetic behaviors of Ni, Co and Fe complexes are reported in Fig. 17. In the three cases the χT product increases when the temperature is decreased and shows a maximum at low temperature. These behaviors indicate the presence of

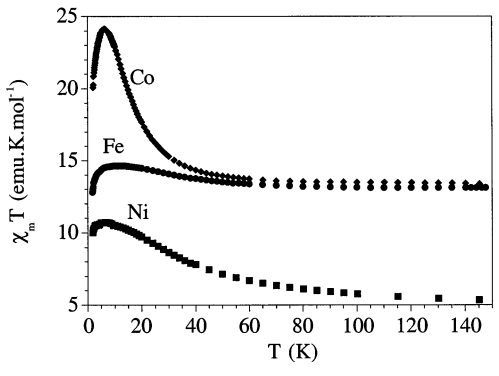

Fig. 17. Magnetic behavior of the Co(II), Fe(II) and Ni(II) complexes of the series $[M_4(H_2O)_2(PW_9O_{34})_2]^{10-}$.

ferromagnetic interactions between the metal ions. Among these compounds, only the Ni_4 cluster allows a proper description of the ground state in terms of the total spin values. Thus, a ferromagnetic coupling between the four local spins $S = 1$ leads to a ground state $S = 4$. In turn, for Co_4 and Fe_4 the presence of an orbital momentum in the ground states of these ions, $^4T_1$ and $^5T_2$, prevents this simple description as the total spin is no longer a good quantum number. A careful analysis of the ground state properties of the Ni_4 and Co_4 clusters has been undertaken. It can be instructive to describe in detail these results as they illustrate how the use of several complementary techniques is essential in order to extract reliable information about the magnetic parameters and to discriminate between physically different models.

For Ni_4 a combination of magnetic susceptibility and magnetization measurements with an INS study has been used to obtain a clear picture of both the magnetic exchange interactions and the spin-anisotropy of the cluster. The bulk magnetic susceptibility has provided information about the sign of the exchange interactions but has shown to be largely insensitive to their values, in particular to the pairwise interaction along the diagonal of the rhomb, J'. In fact, an isotropic Heisenberg model (Eq. (3)) has allowed us to reproduce the magnetic behavior down to 15 K from several set of parameters with J' comprised between 0 and 5 cm^{-1}, while J remains within the range 6.2–7.0 cm^{-1} (dotted line of Fig. 18) [23]. This insensitivity of the magnetic susceptibility to J' is a consequence of the topology of the cluster which leads to an energy spectrum wherein the energy gap between the ground spin level ($S = 4$) and the first excited level ($S = 3$) is equal to $4J$, independent of J' (Fig. 19). To reproduce the maximum in χT, observed at 6 K, and the sharp decrease observed at lower temperatures it has been necessary to

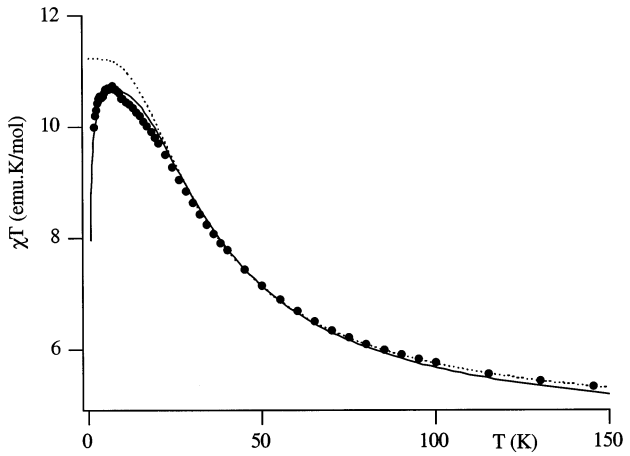

Fig. 18. Magnetic behavior of the Ni(II) complex of the series $[M_4(H_2O)_2(PW_9O_{34})_2]^{10-}$. Dotted line represents the best fit to the isotropic Heisenberg exchange model. Solid line represents the best fit to a model that also considers a single-ion anisotropy term. The resulting parameters are given in the text and in Table 1.

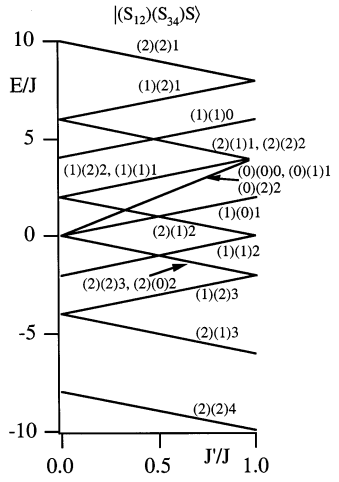

Fig. 19. Energies of the spin states of a rhomb-like cluster of ferromagnetically coupled $S = 1$ spins as a function of the J'/J ratio. The wave functions are labeled according to the Kambe-type coupling scheme (S_{12} and S_{34} are intermediate spin values and S is the total spin).

supplement the isotropic spin Hamiltonian with a zero-field-splitting term that accounts for the Ni(II) spin-anisotropy. Owing to the two kinds of octahedral sites present in the cluster, two different ZFS parameters D and D' have been considered:

$$H_{\mathrm{ZFS}} = D(S_{z1}^2 + \mathrm{S}_{z2}^2) + D'(S_{z3}^2 + S_{z4}^2) \tag{4}$$

However, the magnetic susceptibility only allows us to obtain a rough estimate of the averaged ZFS parameter $\bar{D}(=(D+D')/2)$, which is in the range 2–5 cm^{-1} (solid line of Fig. 18). A more accurate determination of this spin-anisotropy has been extracted from the low temperature magnetization measurements (Fig. 20). They have allowed us to obtain an accurate value of the zero-field-splitting of the $S = 4$ ground spin state of the cluster, which is directly connected with $\bar{D}$. From these measurements we have obtained $\bar{D} = 4.37$ cm^{-1}. However, these measurements do not provide any information on the local D values since information on the splitting of the excited spin multiplets is also required for that purpose. A spectroscopic technique such as the INS has enabled, in addition to more precise information of the $S = 4$ ground-multiplet splitting, the determination of excited spin multiplets [36]. To illustrate the look of the magnetic excitations observed by INS we have plotted the spectra at 1.7, 6 and 15 K obtained on a deuterated sample with an incident neutron wavelength of 6.5 Å that allowed us to cover an energy-transfer range from -1.2 to 1.2 meV ($= 9.6$ cm^{-1}). In this energy range up to four transitions are observed (I–IV) that correspond to the four allowed excitations within the $S = 4$ ground-multiplet (Fig. 21a). By using neutrons with lower wavelengths (2.44, 4.1 and 5.9 Å), magnetic transitions from the ground-multiplet to the excited spin multiplets with $S = 3$ have been observed. They are

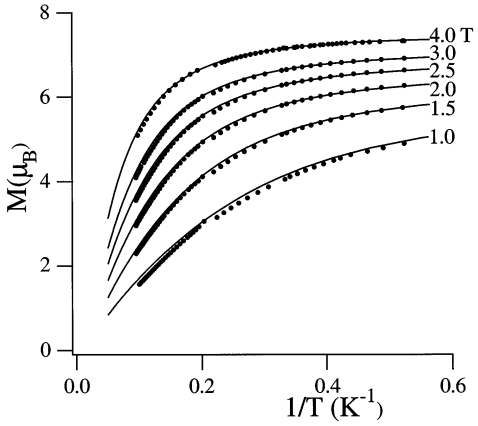

Fig. 20. Magnetization curve vs. the inverse of the temperature for the Ni(II) complex of the series $[M_4(H_2O)_2(PW_9O_{34})_2]^{10-}$ at different magnetic fields. The solid line represents the calculated behavior with the magnetic parameters given in the text.

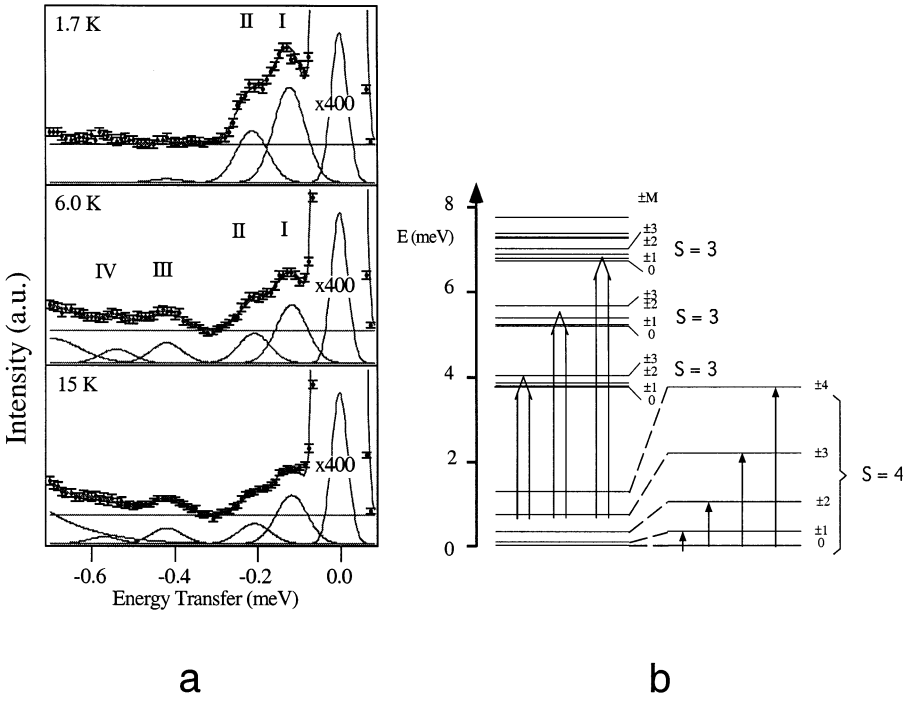

Fig. 21. (a) Inelastic neutron scattering spectra of the deuterated sample $K_6Na_4[Ni_4(H_2O)_2(PW_9O_{34})_2{\cdot}24H_2O$ measured on IN5 at ILL, Grenoble, France, with an incident neutron wavelength of 6.5 Å at temperatures of 1.7, 6.0 and 15 K; (b) energy spectrum of the Ni_4O_{16} ferromagnetic cluster indicating the allowed magnetic excitations.

centered at 3.6, 5.1 and 7.0 meV. From this information an experimental energy-level diagram is derived (Fig. 21b) which can be well reproduced from the Heisenberg spin Hamiltonian supplemented with the ZFS term (Eqs. (3) and (4)). The resulting parameters are $J = 6.7\ cm^{-1}$, $J' = 3.1\ cm^{-1}$, $D = 3.8\ cm^{-1}$ and $D' = 4.9\ cm^{-1}$. They are summarized in Table 1. A reliable value of J' is then obtained by this technique, as well as the values of the two individual single-ion anisotropies. Notice that these D values give an averaged value $\bar{D} = 4.32\ cm^{-1}$, in fair agreement with that derived from magnetization measurements. Further, the fact of obtaining D' larger than D is consistent with the stronger distortion of the hydrated octahedral site.

A more complex situation is provided by the Co_4 cluster as the difficulties associated with the exchange topology of the cluster, already emphasized in the Ni_4 cluster, are accentuated by the fact that the exchange interactions are expected to be largely anisotropic due to the highly anisotropic ground state of octahedral Co(II). In this case the information content of the magnetic susceptibility is clearly insufficient for the determination of the exchange splitting pattern of the ground state of the cluster. In fact, the effective spin Hamiltonian appropriate to fit the magnetic susceptibility data should consider a minimum of eight parameters namely:

(1) four exchange parameters J_z, J_{xy}, J'_z, J'_{xy} to account for the two different exchange pathways J and J' (through the sides and through the diagonal of the rhomb), each one submitted to an axial anisotropy.

(2) four Landé parameters g_z, g_{xy}, g'_z, g'_{xy} to account for the two different anisotropic Co(II) sites.

A fitting of the magnetic data to the above model indicates that this technique can only provide reliable information on the sign of the exchange interactions being almost insensitive to the presence of two different exchange pathways and to the amount of exchange anisotropy [37]. Much more information is obtained from INS measurements performed on fully deuterated samples [38]. The spectrum shows up to six cold peaks which correspond to six magnetic excitations from the ground state to excited states of the tetramer (Fig. 22a). From these data an energy splitting pattern can be obtained (Fig. 22b), which is closely reproduced by an axial-anisotropic exchange model (Eq. (5)) with the parameters $J_z = 10.2\ cm^{-1}$, $J_{xy} = 4.21\ cm^{-1}$, $J'_z = 4.04\ cm^{-1}$, $J'_{xy} = 0.87\ cm^{-1}$. However, this solution completely fails in reproducing the intensities of the observed transitions, despite the excellent reproduction of the energy-level pattern. In particular, transitions II and IV are forbidden by the selection rules as they involve an excitation from the $M = \pm 2$ ground level to $M = 0$ excited levels. An alternative model that solves this problem has been found that assumes a rhombic-anisotropy for the exchange (with $J_z \neq J_x \neq J_y$) [39]. This model reproduces both the energy-level patterns and the observed intensities with the parameters $J_z = 12.2$, $J_x = 5.6$, $J'_z = 3.7$ and $J'_x = 3.5\ cm^{-1}$, $J_x/J_y = J'_x/J'_y = 1.6$. These parameters are summarized in Table 1. Notice that both the axial and the rhombic solutions are equally able to reproduce the bulk properties (magnetic susceptibility, magnetization and magnetic specific heat), as these properties are sensitive to the energy level pattern of the magnetic cluster but not to the nature of the wave functions. At this point, the power of INS compared to these

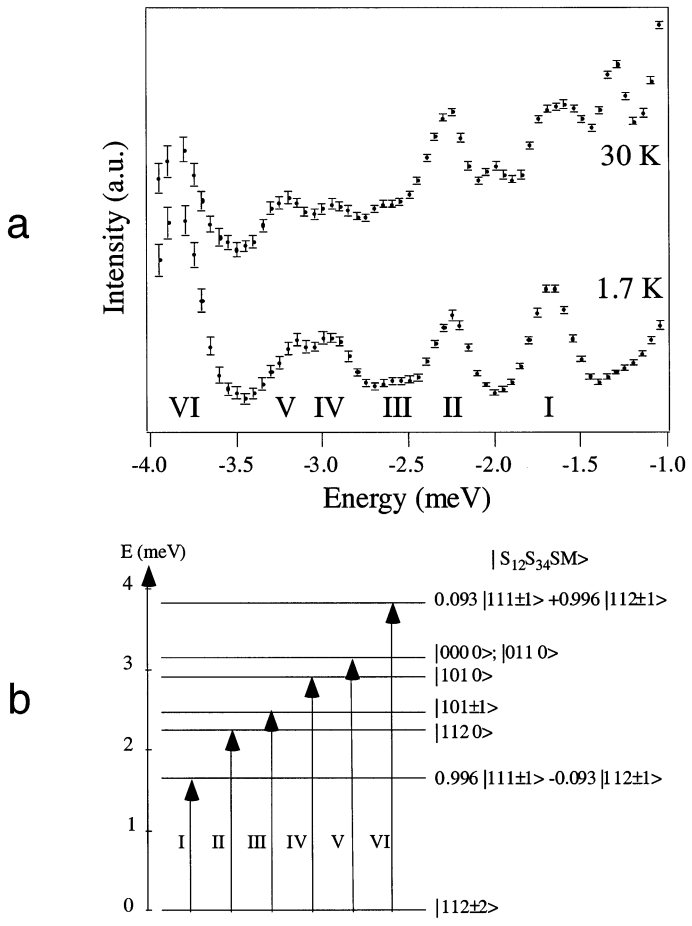

Fig. 22. (a) Inelastic neutron scattering spectra of the deuterated sample $K_{10}[Co_4(H_2O)_2(PW_9O_{34})_2]\cdot 22H_2O$ measured on IN6 at ILL, Grenoble, France, with an incident neutron wavelength of 4.1 Å at 1.7, 10 and 30 K; (b) energy spectrum of the CO_4O_{16} ferromagnetic cluster derived from the INS experiments. Arrows correspond to the observed transitions. The wave functions are those resulting from an exchange model that assumes axial anisotropy (see text).

bulk techniques becomes manifest. With this spectroscopic technique evidence for an exchange-anisotropy in the Co_4 cluster is thus clearly demonstrated for the first time, as well as the validity of using an anisotropic exchange Hamiltonian acting on the basis of the effective spins $S = 1/2$ to model the exchange interactions between high-spin octahedral Co(II) ions.

$$\begin{aligned} H = & -2J_z(S_{z1}S_{z3} + S_{z1}S_{z4} + S_{z2}S_{z3} + S_{z2}S_{z4}) - 2J'_zS_{z1}S_{z2} \\ & - 2J_{xy}(S_{x1}S_{x3} + S_{x1}S_{x4} + S_{x2}S_{x3} + S_{x2}S_{x4} + S_{y1}S_{y3} + S_{y1}S_{y4} + S_{y2}S_{y3} \\ & + S_{y2}S_{y4}) - 2J'_{xy}(S_{x1}S_{x2} + S_{y1}S_{y2}) \end{aligned} \quad (5)$$

2.5. Higher nuclearity magnetic clusters

2.5.1. The series $[M_9(OH)_3(H_2O)_6(HPO_4)_2(PW_9O_{34})_3]^{16-}$ (M(II) = Ni, Co)

These two complexes, abbreviated as Ni_9 and Co_9, represent the highest nuclearity magnetic clusters so far obtained from the trivacant polytungstate ligand B-$[PW_9O_{34}]^{9-}$. In these nonanuclear magnetic clusters the exchange pathways are more complex than in the previous cases as they involve not only the oxo bridges but also the two central HPO_4^{2-} groups. However, the ability of this group to propagate exchange interactions is small compared to that of the μ-oxo groups. Neglecting this pathway, the presence of two types of connections between the MO_6 octahedra should lead to two types of exchange interactions as schematized in Fig. 23(a): the intra-triangle exchange, J, associated with the pairwise interactions within the M_3 edge-sharing clusters from each Keggin sub-unit, and the inter-triangle exchange, J', that accounts for the M–O–M connections between different M_3 triangles. Since this last involves corner-sharing MO_6 octahedra with M–O–M angles around 120° or even larger, this exchange pathway should be antiferromagnetic. Therefore, unprecedented magnetic clusters showing coexistence of both ferro- and antiferromagnetic couplings are to be expected. The magnetic properties of Ni_9 confirm this prediction (Fig. 23b) [22]. The increase in χT down to 30 K indicates the presence of dominant ferromagnetic interactions within the triangles, while the sharp decrease at lower temperatures is a consequence of the antiferromagnetic inter-triangle interactions. The quantitative analysis of the magnetic properties of this cluster is not an easy task as the overall spin states to be considered are $3^9 = 19\,683$. This has imposed the use of a fully isotropic Hamiltonian, neglecting thus single-ion anisotropy effects. A good reproduction of the experiment has been obtained with $J = 3.9$ and $J' = -1.4$ cm^{-1} (solid line in Fig.

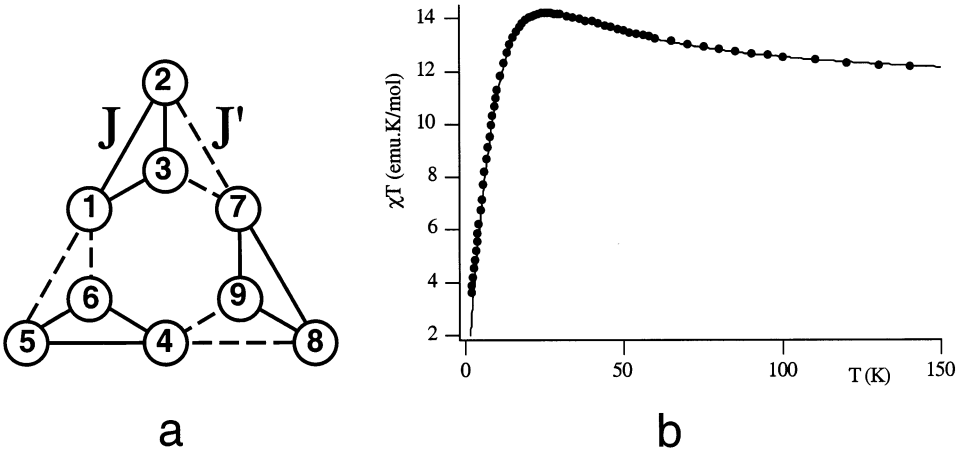

Fig. 23. (a) Exchange network in the nonanuclear magnetic clusters M_9O_{36} of the series $[M_9(OH)_3(H_2O)_6(HPO_4)_2(PW_9O_{34})_3]^{16-}$ (M(II) = Ni, Co); (b) magnetic behavior of the Ni complex. The solid line represents the best fit to the isotropic Heisenberg model (see Table 1).

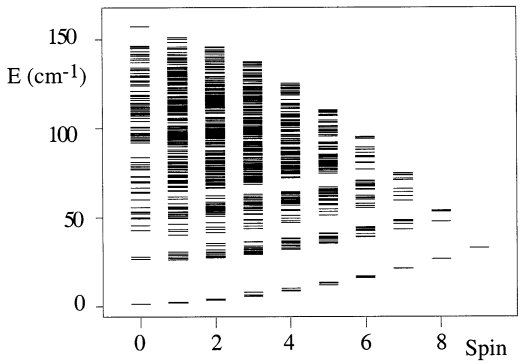

Fig. 24. Calculated spin levels of the Ni_9 cluster.

23b; Table 1). Due to the presence of an antiferromagnetic interaction, the lower spin states of the cluster are stabilized in such a way that the $S = 0$ spin state becomes the ground state of the cluster. An interesting result of this analysis is that the ferromagnetic intra-triangle exchange parameter, J, compares quite well with those obtained in Ni_3 and Ni_4 clusters (see Table 1). This confirms the validity of the models and of the magneto-structural correlations in these Ni clusters. Another important feature of Ni_9 concerns its energy spectrum (Fig. 24). As can be seen it is in between that of a small cluster (like Ni_3), characterized by the presence of discrete levels, and that of an infinite solid, characterized by the presence of energy bands formed by a continuum of energy levels. The lowest lying energy levels of Ni_9 are well separated in energy one from the other and therefore, quantum effects should be still present for this nuclearity.

As for Ni_9, in Co_9 a coexistence of ferro- and antiferromagnetic interactions is to be expected. In this case, however, the χT product shows a continuous decrease when the temperature is decreased (Fig. 25). This may be consistent with the

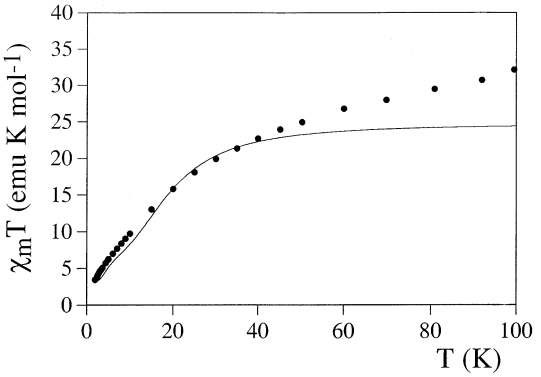

Fig. 25. Magnetic behavior of the $[Co_9(OH)_3(H_2O)_6(HPO_4)_2(PW_9O_{34})_3]^{16-}$ complex. The solid line represents the best fit to the anisotropic Ising exchange model (see Table 1).

presence of dominant antiferromagnetic interactions. In fact, a quantitative analysis of the data in the low temperature region (below 30–40 K) using a fully anisotropic Ising Hamiltonian gives a ferromagnetic intra-triangle interaction $J_z = 8.4$ cm^{-1}, and a stronger and antiferromagnetic inter-triangle interaction $J'_z = -12$ cm^{-1} [40] (solid line in Fig. 25). As can be seen in Table 1 the ferromagnetic exchange parameter compares quite well with that obtained in Co_4 cluster.

2.5.2. Other magnetic clusters with nuclearities larger than 4

Very few examples of heteropoly complexes containing clusters of this kind have been so far magnetically characterized. Of nuclearity 5 we can mention the complex $[WCo_3(H_2O)_2(CoW_9O_{34})_2]^{12-}$ that comprises a central rhomb-like cluster containing a trimeric Co_3 cluster of edge-sharing CoO_6 octahedra connected by oxo groups to two tetrahedral CoO_4 units belonging to the two $\{CoW_9\}$ moieties (Fig. 10a) [25]. Magnetically this cluster may be viewed as a hybrid between the tetrameric cluster encapsulated in the complex $[Co_4(H_2O)_2(PW_9O_{34})_2]^{10-}$ and the Co(II)Co(II) dimer present in $[Co(H_2O)CoW_{11}O_{39}]^{8-}$. In the former the exchange pathways involve edge-sharing CoO_6 octahedra, while in the second they involve an octahedral Co(II) site connected to a tetrahedral Co(II) site through a common oxo group. Accordingly, the magnetic properties have been analyzed taking into account these two kinds of exchange interactions [41]. The best fit to an anisotropic exchange model gives as exchange parameters: a ferromagnetic and anisotropic exchange interaction between the octahedral cobalt's, $J_z = 12.2$ and $J_{xy} = 5.6$ cm^{-1}; and an antiferromagnetic and anisotropic interaction for the octahedral–tetrahedral cobalt pairs, $J_z = -10.0$ and $J_{xy} = -3.3$ cm^{-1} (Fig. 26). Despite the overparametrization in the fitting procedure, these values predict the right sign and magnitude of the exchange parameters being in good agreement with those obtained in the two related clusters, Co_4 and Co_2 (see Table 1).

An example of nuclearity 6 is provided by the complex $[Fe_2Cu_2(H_2O)_2(FeW_9O_{34})_2]^{12-}$. This anion contains a central cluster $Fe(III)_2Cu(II)_2$

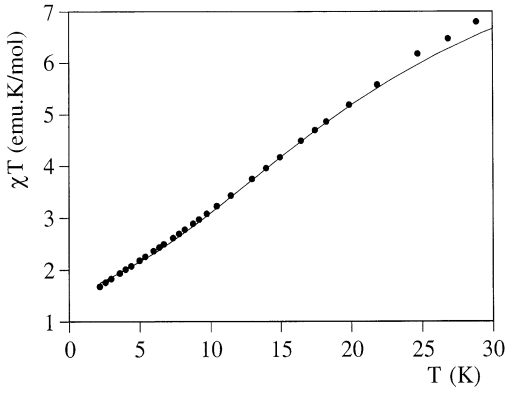

Fig. 26. Low temperature magnetic behavior of the complex $[WCo_3(H_2O)_2(CoW_9O_{34})_2]^{12-}$. The solid line represents the best fit to an anisotropic exchange model (see Table 1).

connected to two tetrahedral Fe(III) ions through an oxo bridge (Fig. 10b). The magnetic properties indicate the presence of significant antiferromagnetic interactions [26]. No attempt to quantitatively analyze these properties has been made so far.

3. Mixed-valence clusters

Polyoxometalates provide unique examples in coordination chemistry of large nuclearity mixed valence clusters in which a variable number of electrons can undergo a rapid electron transfer from one center to the other [6]. For example in the 12-site Keggin structure addition of one or two blue electrons involves hopping among the 12 addenda atoms. In the 18-site Dawson–Wells structure this hopping is restricted to the two internal hexagonal belts. In both structures addition of two blue electrons always results in a complete spin pairing of the electrons at room temperature; consequently, the complexes are diamagnetic. Baker and co-workers in a continuing series of papers examined the blue electron distributions and delocalization in these mixed valence clusters using NMR [42]. They also examined the change in magnetic properties induced by addition of blue electrons in derivatives with Keggin and Dawson–Wells structures containing one or two paramagnetic centers [9]. This feature provided the opportunity for studying the interactions between delocalized electrons and localized magnetic moments at the molecular level.

Motivated by these experimental works, we have explored the problems associated with the interplay between electron delocalization and spin interactions in these large mixed-valence clusters. These problems are of current interest in magnetism due to the possibility of strongly stabilizing a ferromagnetic coupling between the magnetic centers via a special kind of exchange coupling namely double-exchange [43,44], a mechanism that is operative in a variety of mixed valence systems including the clusters of biological relevance [3,4], and the rare-earth manganates exhibiting giant magnetorresistance [45]. Until very recently, however, the interplay between electron delocalization and magnetic interactions was thoroughly treated for dimers, trimers and tetramers, but there was no treatment available for larger clusters [46]. The high symmetries exhibited by the heteropoly complexes allowed us to exploit the group theoretical approach to develop analytical solutions for the energy levels and magnetic properties of these mixed valence clusters. In this context, we have examined the problem of electron delocalization and spin coupling in the two-electron reduced heteropoly blues with Keggin [47] and Dawson–Wells structures [48]. The model considers the Coulomb interactions between the two blue electrons that tend to keep these electrons on fairly widely separated metal sites, and the single- and double-electron transfer processes that occur through the corners or through the edges of neighboring octahedral metal sites promoting the electron delocalization. The problem of localization–delocalization of this electronic pair, as well as its electron distribution within the cluster, has also been examined by introducing the vibronic interactions

[49]. The main conclusion of our model is that electron delocalization is at the origin of the spin pairing of the two electrons, as these transfer processes are operative even when the two blue electrons are widely separated in the polyoxometalate framework to minimize the Coulomb energy. It is precisely the simultaneous effect of these two transfer processes combined with the Coulomb repulsion that accounts for the energetic stabilization of the spin singlet with respect to the spin triplet. In fact, an oversimplified model that only considers the single-transfer processes leads to a highly degenerate ground spin state formed by an extensive mixture of singlets and triplets [50]. Our model makes it unnecessary to involve a multiroute superexchange mechanism in order to explain the very strong antiferromagnetic coupling observed in all polyoxometalates reduced by even numbers of delocalized electrons. Recently, a model of this kind has also been worked out to study the electron delocalization in the two-electron reduced decatungstate $[W_{10}O_{32}]^{6-}$ [51].

A variant of the theme is provided by the mixed valence clusters $[V_{18}O_{42}]^{n-}$ reported by Müller et al. (Fig. 27) [52]. In these clusters the V(V)/V(IV) ratios can be varied from the fully reduced single-valence cluster $\{V_{18}(IV)\}$ to the partially oxidized mixed-valence cluster $\{V_{10}(IV)V_8(V)\}$. The magnetic properties indicate that the antiferromagnetic coupling is much larger in the latter. This is a surprising result since the mixed-valence cluster comprises a smaller number of magnetic vanadium(IV) centers (10 compared to 18), and thus, one should expect a weakening in the V(IV)–V(IV) interactions on increasing the number of diamagnetic vanadium(V) centers. This stronger coupling has tentatively been attributed to electron-transfer effects. In order to explain such a result in a more convincing way, we have developed a model that considers the electron-transfer processes from V(IV) to V(V) centers, the exchange interactions between the V(IV) centers, and the Coulomb repulsion parameter preventing two electrons being on the same site [53].

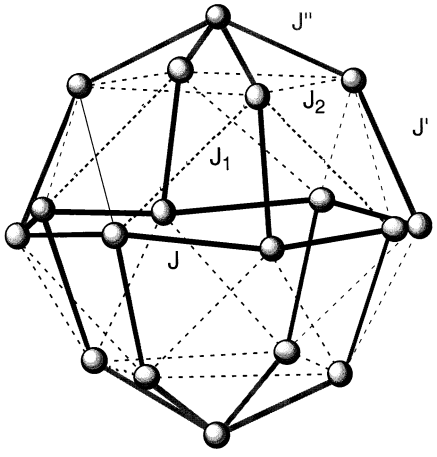

Fig. 27. Polyhedron describing the structure of the $\{V_{18}O_{42}\}$ species and scheme of the possible important exchange pathways: $J \approx J' \sim 200\ cm^{-1}$; $J_1 \approx J_2 \sim 80\ cm^{-1}$; $J'' \sim 50\ cm^{-1}$.

Notice that from the theoretical point of view, this problem is much more difficult than that encountered in the two-electron reduced Keggin and Dawson–Wells polyoxometalates. In fact, one pass from a system formed by two delocalized electrons undergoing electron-transfer processes among 12 metal sites, to a system formed by ten delocalized electrons undergoing electron-transfer processes among 18 metal sites, as well as magnetic exchange interactions when they are on adjacent sites. A general computing approach recently developed in our group has been used to treat the system [54]. Since the rigorous procedure would require prohibitively large matrices to diagonalize and long computer times, we have considered a model system that comprises ten metal sites and six delocalized electrons (Fig. 28). The evolution of the lower-lying spin levels with the transfer parameter t is reported in the Figure. One observes that the electron delocalization results in a strong stabilization of the antiferromagnetic ground state with respect to the fist excited spin-triplet level. This analysis provides theoretical support to the experimental findings.

4. Concluding remarks

In this review we have illustrated the richness of polyoxometalate chemistry in providing ideal examples of magnetic and mixed-valence clusters of increasing

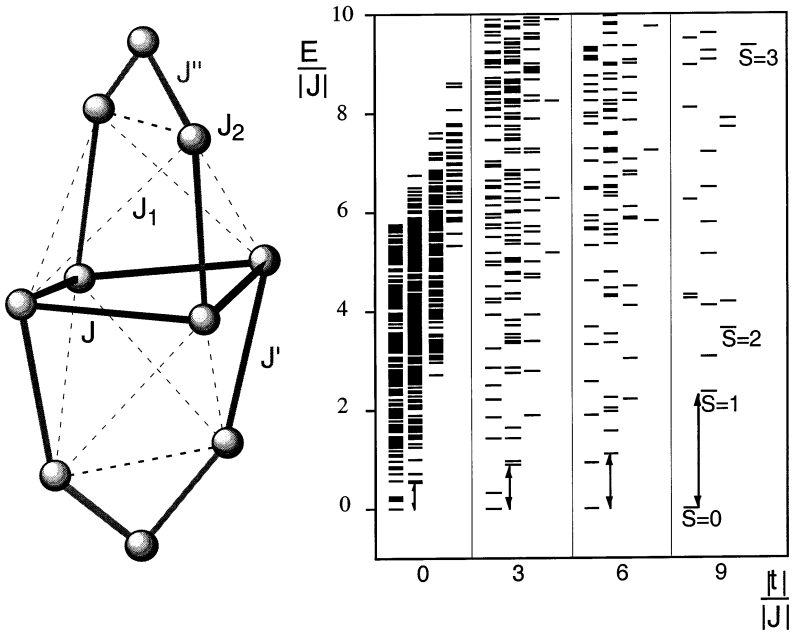

Fig. 28. Polyhedral model used to calculate the spin levels of the partially oxidized mixed-valence cluster $\{V_{10}(IV)V_8(V)O_{42}\}$ (right). Influence of the electron transfer on the lower lying spin levels of the mixed-valence cluster showing the stabilization of the $S = 0$ spin state as the electron delocalization is increased.

nuclearities and topological and electronic complexities. As pointed out in the introduction and demonstrated along the work, an interesting combination of chemical, structural and electronic features make these complexes very suitable as model systems in molecular magnetism. For example, highly-insulated magnetic clusters with prearranged topologies and nuclearities, having predictable and often ferromagnetic exchange interactions, can be obtained with a variety of paramagnetic metal ions. This is exemplified by the nickel(II) clusters obtained from the phosphotungstate ligand. This heptadentate rigid ligand allows us to increase the number of exchange-coupled magnetic centers from 3 to 9 using preformed building blocks. In all cases a basic triangular cluster, formed by three edge-sharing NiO_6 octahedra, is maintained. In Ni_3 and Ni_4 the presence of this basic unit leads to ferromagnetic interactions, and therefore, to the stabilization of the higher spin states, $S = 3$ and $S = 4$, respectively, which become the ground spin states of these clusters. On the other hand, the coexistence in Ni_9 of NiO_6 octahedra sharing edges and corners leads to a coexistence of competing ferromagnetic and antiferromagnetic interactions, which results in a non magnetic ground spin state.

Compared to other polymetallic complexes, several reasons justify the magnetic interest for these metal–oxide clusters:

- From the experimental point of view, the thorough characterization of the ground state properties in a magnetic cluster is essential for in-depth understanding of the magnetic exchange interaction phenomenon. As the complexity of the cluster increases, the information content of the routine magnetic techniques (magnetic susceptibility, magnetization, EPR) is insufficient for this purpose and other complementary techniques become crucial. The magnetic clusters encapsulated by polyoxotungstate ligands are revealing examples of this statement. Thus, the possibility of having large amounts (10–20 g) of fully deuterated salts of these polyoxometalates available, has enabled the use of INS, a spectroscopic technique that provides direct information on the energy splitting pattern caused by exchange interactions. Just to mention a relevant result, the first direct evidence of exchange-anisotropy in cobalt(II) clusters has been clearly demonstrated by INS in the polyoxometalates $[Co(H_2O)CoW_{11}O_{39}]^{8-}$ and $[Co_4(H_2O)_2(PW_9O_{34})_2]^{10-}$. Despite the power of this technique, the sample requirements (deuteration and big amounts of sample) have restricted its use in coordination chemistry. The advantage of polyoxometalate complexes in this respect is obvious.
- From the theoretical point of view, the high symmetry of the cluster, imposed by the polyoxometalate framework, has facilitated the development of exact quantum-mechanical models from which a clear picture of the relevant parameters involved in the magnetic properties can be extracted. This has been particularly useful for the treatment of the mixed-valence polyoxometalates. In this context, polyoxometalates represent a step forward from the simple mixed-valence clusters of nuclearities 2, 3 and 4 so far investigated [46]. They possess the largest nuclearities and most complex topologies ever seen for clusters in the mixed-valence area. Therefore, the quantitative interpretation of the magnetic properties

of these systems is a challenging problem, as they are often too complex to be treated with the existing theories. However, exact solutions have been developed in some cases that provide important hints on the role played by the electron transfer processes on the magnetic properties of these clusters. For example, it has been shown that in these structures, electron delocalization can result in a strong antiferromagnetic coupling between widely separated blue electrons. Notice that even when exact solutions are available, the large number of parameters involved in the electronic processes—transfer and exchange parameters—strongly limits the correct analysis of the experimental data and independent information about the sign and magnitude of these parameters then becomes crucial. In the future, molecular orbital calculations should be a useful tool in this context.

To finish we would like to mention two more aspects of potential interest in connection with the magnetic polyoxometalates:

- One refers to the possibility of polyoxometalates acting as bridging ligands to form polymeric complexes. Although examples of extended heteropolyanions showing chain- or layer-like networks are scarce, these kinds of structures may provide novel types of low-dimensional magnetic materials. For example the infinite linear chain polyanion $[MnPW_{11}O_{39}]^{5-}$ present in the hybrid salt $[ET]_8[MnPW_{11}O_{39}]$ (ET = bis(ethylenedithio)tetrathiafulvalene) [55]. The formation of this chain involves a condensation of monosubstituted Keggin anions $[Mn(H_2O)PW_{11}O_{39}]^{5-}$, with the subsequent displacement of the molecule of water coordinated to Mn(II) in one Keggin unit by a terminal oxygen atom on W in another unit. As a result, the Keggin units are linked by a common oxo-bridge that connects a W atom with a Mn one (Fig. 29). From the magnetic point of view the paramagnetic Mn(II) centers are independent, as they are separated by the diamagnetic undecatungstate anion. However, an original magnetic situation should be expected when blue electrons are injected in the polyoxometalate, as in this case localized spins and itinerant electrons can coexist and interact within the resulting mixed-valence chain [56]. This provides the unique opportunity to look for the presence of an indirect magnetic coupling between Mn(II), which are more than 11 Å away, via the itinerant blue electrons. Some evidence for this coupling has been found in the reduced molybdenum derivative.

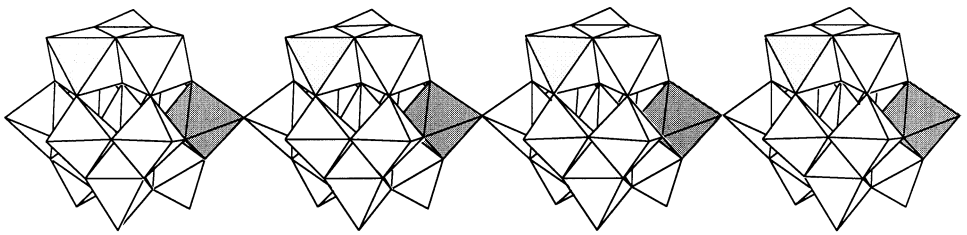

Fig. 29. Structure of the infinite linear chain polyanion $[MnPM_{11}O_{39}]^{5-}$ (M = W, Mo).

- The other aspect of interest is related to the possibility of using these molecular anions as magnetic components of novel molecular and polymeric materials with interesting physical properties or combination of properties. Thus, they have been combined with organic donors of the tetrathiafulvalene (TTF) type to form radical salts with coexistence of localized magnetic moments and itinerant electrons [57]. On the other hand, they have been embedded in conducting polymers such as polypyrrole to form hybrid functional films [58]. Finally, they have been incorporated into Langmuir–Blodgett films to produce organic–inorganic hybrids containing well-organized monolayers of polyoxometalates, separated by bilayers of amphiphilic lipid molecules [59].

Acknowledgements

We wish to thank our colleagues, co-workers and collaborators for the important contributions to the work reported herein, in particular the Valencia group (J.J. Borrás-Almenar, M. Clemente-León, J.R. Galán-Mascarós, C.J. Gómez-García, A.V. Palii and B.S. Tsukerblat) and the Bern group (M. Aebersold, H. Andres and H.U. Güdel). Financial support by the Spanish Ministerio de Educación y Cultura (Grant PB96-0862) is gratefully acknowledged. J.M.C.-J. thanks the Generalitat Valenciana for a predoctoral grant.

References

[1] (a) D. Gatteschi, A. Caneschi, L. Pardi, R. Sessoli, Science 265 (1994) 1054. (b) L. Thomas, F. Lionti, R. Ballou, D. Gatteschi, R. Sessoli, B. Barbara, Nature 383 (1996) 145. (c) H.J. Eppley, H.L. Tsai, N. de Vries, G. Christou, D.N. Hendrickson, J. Am. Chem. Soc. 117 (1995) 301. (d) R. Sessoli, H.L. Tsai, A.R. Schake, S. Wang, J.B. Vincent, K. Folting, D. Gatteschi, G. Christou, D.N. Hendrickson, J. Am. Chem. Soc. 115 (1993) 1804. (e) S.M.J. Aubin, Z. Sun, I.A. Guzei, A.L. Rheingold, G. Christou, D.N. Hendrickson, Chem. Commun. (1997) 2239. (f) J. Friedman, M. Sarachik, J. Tejada, R. Ziolo, Phys. Rev. Lett. 76 (1996) 3830.
[2] (b) I. Fujita, Y. Yeki, T. Takui, T. Kinoshita, K. Itoh, F. Miko, Y. Sawaki, H. Iwamura, A. Izuoka, T. Sugawara, J. Am. Chem. Soc. 112 (1990) 4074. (b) T. Ishida, H. Iwamura, J. Am. Chem. Soc. 113 (1991) 4238. (c) N. Nakamura, K. Inoue, H. Iwamura, Angew. Chem. Int. Ed. Engl. 32 (1993) 873. (d) N. Ventosa, D. Ruiz, C. Rovira, J. Veciana, Mol. Cryst. Liq. Cryst. 232 (1993) 333. (e) A. Rajca, S. Utamapanya, S. Thayumanavan, J. Am. Chem. Soc. 114 (1992) 1884.
[3] G. Blondin, J.J. Girerd, Chem. Rev. 90 (1989) 1359.
[4] G. Christou, Acc. Chem. Res. 22 (1989) 328.
[5] (A) S.J. Lippard, Angew. Chem. Int. Ed. Engl. 30 (1991) 34. (b) G.C. Papaefthymiou, S.J. Lippard, Inorg. Chem. 33 (1994)1510.
[6] An updated revision of the state-of-the-art in this area can be found in (a) C.L. Hill (Ed.), Polyoxometalates, Chem. Rev. 98 (1998). (b) M.T. Pope, A. Müller (Eds.), Polyoxometalates: From Platonic Solids to Anti-Retroviral Activity, Kluwer Academic Publishers, Dordrecht, 1994.
[7] E. Coronado, C.J. Gómez-García, Comments Inorg. Chem. 17 (1995) 255.
[8] M.T. Pope, Heteropoly and Isopoly Oxometalates, Springer-Verlag, Berlin, 1983.
[9] (a) N. Casañ-Pastor, L.C.W. Baker, J. Am. Chem. Soc. 114 (1992) 10384. (b) N. Casañ-Pastor, L.C.W. Baker, in: M.T. Pope, A. Müller (Eds.), Polyoxometalates: From Platonic Solids to Anti-Retroviral Activity, Kluwer Academic Publishers, Dordrecht, 1994, p. 203.

[10] (a) D. Gatteschi, L. Pardi, A.L. Barra, A. Müller, in: M.T. Pope, A. Müller (Eds.), Polyoxometalates: From Platonic Solids to Anti-Retroviral Activity, Kluwer Academic Publishers, Dordrecht, 1994, p. 219. (b) A. Müller, F. Peters, M.T. Pope, D. Gatteschi, Chem. Rev. 98 (1998) 239.
[11] (a) L.C.W. Baker, V.E.S. Baker, S.H. Wasfi, G.A. Candela, A.H. Kahn, J. Am. Chem. Soc. 94 (1972) 5499. (b) L.C.W. Baker, V.E.S. Baker, S.H. Wasfi, G.A. Candela, A.H. Kahn, J. Chem. Phys. 56 (1972) 4917.
[12] (a) W.H. Knoth, P.J. Domaille, R.D. Farlee, Organometallics 4 (1985) 62. (b) W.H. Knoth, P.J. Domaille, R.L. Harlow Inorg. Chem. 25 (1986) 1577.
[13] F. Robert, M. Leyrie, G. Hervé, Acta Crystallogr. Sect. B G38 (1982) 358.
[14] (a) T.J.R. Weakley, H.T. Evans, J.S. Showell, G.F. Tourné, C.M. Tourné, J. Chem. Soc. Chem. Commun. (1973) 139. (b) H.T. Evans, C.M. Tourné, G.F. Tourné, T.J.R. Weakley, J. Chem. Soc. Dalton Trans. (1986) 2699.
[15] R.G. Finke, M.W. Droege, P.J. Domaille, Inorg. Chem. 26 (1987) 3886.
[16] T.J.R. Weakley, R.G. Finke, Inorg. Chem. 29 (1990) 1235.
[17] C.J. Gómez-García, E. Coronado, P. Gómez-Romero, N. Casañ-Pastor, Inorg. Chem. 32 (1993) 3378.
[18] X.Y. Zhang, G.B. Jameson, C.J. O'Connor, M.T. Pope, Polyhedron 15 (1996) 917.
[19] X.Y. Zhang, Q. Chen, D.C. Duncan, R.J. Lachiotte, C.L. Hill, Inorg. Chem. 36 (1997) 4381.
[20] C.J. Gómez-García, J.J. Borrás-Almenar, E. Coronado, L. Ouahab, Inorg. Chem. 33 (1994) 4016.
[21] C.J. Gómez-García, E. Coronado, P. Gómez-Romero, N. Casañ-Pastor, Inorg. Chem. 32 (1993) 89.
[22] J.M. Clemente-Juan, E. Coronado, J.R. Galán-Mascarós, C.J. Gómez-García, Inorg. Chem. 38 (1999) 55.
[23] C.J. Gómez-García, E. Coronado, L. Ouahab, Angew. Chem. Int. Ed. Engl. 31 (1992) 649.
[24] T.J.R. Weakley, J. Chem. Soc. Chem. Commun. (1984) 1406.
[25] C.M. Tourné, G.F. Tourné, F. Zonnevijlle, J. Chem. Soc. Dalton Trans. (1991) 143.
[26] S.H. Wasfi, A.L. Rheingold, G.F. Kokoszka, A.S. Goldstein, Inorg. Chem. 26 (1987) 2934.
[27] (a) H.U. Güdel, A. Furrer, Mol. Phys. 5 (1977) 1335. (b) H.U. Güdel, in: E. Coronado, P. Delhaes, D. Gatteschi, J.S. Miller (Eds.), Molecular Magnetism: From Molecular Assemblies to the devices, Kluwer A.P, Dordrecht, 1996, NATO ASI Series E, vol. 321, p. 229.
[28] H. Andres, M. Aebersold, H.U. Güdel, J.M. Clemente, E. Coronado, H. Büttner, G. Kearly, M. Zolliker, Chem. Phys. Lett. 289 (1998) 224.
[29] R.L. Carlin, Magnetochemistry, Springer, New York, 1986.
[30] G.F. Kokoszka, F. Padula, A.S. Goldstein, E.L. Venturini, L. Azevedo, A.R. Siedle, Inorg. Chem. 27 (1988) 59.
[31] A.R. Siedle, F. Padula, J. Baranowski, A.S. Goldstein, M. DeAngelo, G.F. Kokoszka, L. Azevedo, E.L. Venturini, J. Am. Chem. Soc. 105 (1983) 7447.
[32] J.A. Bertrand, A.P. Ginsberg, R.I. Kaplan, C.E. Kirkwood, R.L. Martin, R.C. Sherwood, Inorg. Chem. 10 (1971) 240.
[33] C.J. Gómez-García, N. Casañ-Pastor, E. Coronado, L.C.W. Baker, G. Pourroy, J. Appl. Phys. 67 (1990) 5995.
[34] C.J. Gómez-García, E. Coronado, J.J. Borrás-Almenar, Inorg. Chem. 31 (1992) 1667.
[35] J.K. McCuster, E.A. Schmitt, D.N. Hendrickson, in: D. Gatteschi, O. Kahn, J.S. Miller, F. Palacio (Eds.), Magnetic Molecular Materials, vol. E 198, NATO ASI Series, Kluwer Academic Publishers, 1991, p. 297.
[36] J.M. Clemente-Juan, H. Andres, J.J. Borrás-Almenar, E. Coronado, H.U. Güdel, M. Aebersold, G. Kearly, Herma Büttner, M. Zolliker, J. Am. Chem. Soc., in press.
[37] N. Casañ-Pastor, J. Bas, E. Coronado, G. Pourroy, L.C.W. Baker, J. Am. Chem. Soc. 114 (1992) 10380.
[38] (a) C.J. Gómez-García, E. Coronado, J.J. Borrás-Almenar, M. Aebersold, H.U. Güdel, H. Mutka, Physica B 180–181 (1992) 238. (b) J.M. Clemente-Juan, H. Andres, M. Aebersold, J.J. Borrás-Almenar, E. Coronado, H.U. Güdel, H. Büttner, G. Kearly, Inorg. Chem. 36 (1997) 2244. (c) M. Aebersold, H.P. Andres, H. Büttner, J.J. Borrás-Almenar, J.M. Clemente-Juan, E. Coronado, H.U. Güedel, D. Kearley, Physica B 234–236 (1997) 764.

[39] H. Andres, J.M. Clemente-Juan, M. Aebersold, H.U. Güdel, E. Coronado, H. Büttner, G. Kearly, Julio Melero, R. Burriel, J. Am. Chem. Soc., submitted.
[40] J.R. Galán-Mascarós, C.J. Gómez-García, J.J. Borrás-Almenar, E. Coronado, Adv. Mater. 6 (1994) 221.
[41] J.M. Clemente-Juan, Doctoral Dissertation, University of Valencia, 1998.
[42] M. Kozik, L.C.W. Baker, in: M.T. Pope, A. Müller (Eds.), Polyoxometalates: From Platonic Solids to Anti-Retroviral Activity, Kluwer Academic Publishers, Dordrecht, 1994, p. 191 and references therein.
[43] P.W. Anderson, H. Hasegawa, Phys. Rev. 100 (1955) 675.
[44] E. Coronado, R. Georges, B.S. Tsukerblat, in: E. Coronado, P. Delhaes, D. Gatteschi, J.S. Miller (Eds.), Molecular Magnetism: From Molecular Assemblies to the Devices, vol. E 321, NATO ASI Series, Kluwer Academic Publishers, Dordrecht, 1996, p. 65.
[45] C.N.R. Rao, Chem. Eur. J. 2 (1996) 1499.
[46] J.J. Borrás Almenar, E. Coronado, R. Georges, B.S. Tsukerblat, in: E. Coronado, P. Delhaes, D. Gatteschi, J.S. Miller (Eds.), Molecular Magnetism: From Molecular Assemblies to the Devices, vol. E 321, NATO ASI Series, Kluwer Academic Publishers, Dordrecht, 1996, p. 105.
[47] J.J. Borrás-Almenar, J.M. Clemente, E. Coronado, B.S. Tsukerblat, Chem. Phys. 195 (1995) 1.
[48] J.J. Borrás-Almenar, J.M. Clemente, E. Coronado, B.S. Tsukerblat, Chem. Phys. 195 (1995) 16.
[49] J.J. Borrás-Almenar, J.M. Clemente, E. Coronado, B.S. Tsukerblat, Chem. Phys. 195 (1995) 29.
[50] S.A. Borshch, B. Bigot, Chem. Phys. Lett. 212 (1993) 398.
[51] S.A. Borshch, Inorg. Chem. 30 (1998) 3116.
[52] A. Müller, R. Sessoli, E. Krickemeyer, H. Bögge, J. Meyer, D. Gatteschi, L. Pardi, J. Westphal, K. Hovemeier, R. Rohlfing, J. Döring, I. Hellweg, C. Beugholt, M. Schmidtmann, Inorg. Chem. 36 (1997) 5239.
[53] E. Coronado et al. , unpublished results.
[54] J.J. Borrás-Almenar, J.M. Clemente-Juan, E. Coronado, R. Georges, A.V. Palii, B.S. Tsukerblat, J. Chem. Phys. 105 (1996) 6892.
[55] J.R. Galán-Mascarós, C. Giménez-Saiz, S. Triki, C.J. Gómez-García, E. Coronado, L. Ouahab, Angew. Chem. Int. Ed. Engl. 34 (1995) 1460.
[56] E. Coronado, J.R. Galán-Mascarós, C. Giménez-Saiz, C.J. Gómez-García, S. Triki, J. Am. Chem. Soc. 120 (1998) 4671.
[57] E. Coronado, C.J. Gómez-García, Chem. Rev. 98 (1998) 275.
[58] M. Clemente-León, E. Coronado, J.R. Galán-Mascarós, C. Giménez-Saiz, C.J. Gómez-García, T.F. Otero, J. Mater. Chem. 8 (1998) 309.
[59] (a) M. Clemente-León, B. Agricole, C. Mingotaud, C.J. Gómez-García, E. Coronado, P. Delhaes, Langmuir 13 (1997) 2340. (b) M. Clemente-León, B. Agricole, C. Mingotaud, C.J. Gómez-García, E. Coronado, P. Delhaes, Angew. Chem. Int. Ed. Engl. 36 (1997) 1114.